Available online at www.sciencedirect.com
SCIENCE DIRECT®
Earth-Science Reviews 66 (2004) 63–87
EARTH-SCIENCE REVIEWS
www.elsevier.com/locate/earscirev

Comparing the Epica and Vostok dust records during the last 220,000 years: stratigraphical correlation and provenance in glacial periods

B. Delmonte[a,b,c,*], I. Basile-Doelsch[d,e], J.-R. Petit[a], V. Maggi[b], M. Revel-Rolland[f], A. Michard[d], E. Jagoutz[g], F. Grousset[h]

[a] *Laboratoire de Glaciologie et de Géophysique de l'Environnement, 54, rue Moliere, BP96, 38402, Saint Martin d'Hères, France*
[b] *Department of Geological Science, University of Siena, Via del Laterino 8, 53100, Siena, Italy*
[c] *Dip. Scienze Ambientali, University of Milano-Bicocca, Piazza della Scienza 1, 20126, Milan, Italy*
[d] *CEREGE–CNRS, UMR 6635, Europole Méditerranéen de l'Arbois, BP 80, 13545, Aix en Provence, Cedex 4, France*
[e] *IRD-BP 172 97492 Sainte-Clotilde cedex, France*
[f] *Department of Geology, The Australian National University Canberra, ACT 0200 Australia*
[g] *Cosmochemistry Department, Max Plank Institut fur Chemie, 55020 Mainz, Germany*
[h] *EPOC, CNRS UMR 5805, Université Bordeaux I Ave. des Facultés, 33405 Talence, France*

Received 3 July 2003; accepted 27 October 2003

Abstract

A new aeolian dust record from the first 2200 m of the EPICA-Dome C ice core (75°06′ S, 123°21′ E) covering about 220,000 years of climatic history is compared to the Vostok (78°28′ S, 106°48′ E) ice core [Nature 399 (1999) 429]. The two dust profiles are very similar and several common dust events allow to establish stratigraphical links.

The late Quaternary period is characterized at both sites, and likely overall East Antarctic plateau, by high dust input during glacial periods. In the EPICA-Dome C ice core, the dust flux rises by a factor of ~ 25, ~ 20 and ~ 12 in glacial stages 2, 4 and 6 with respect to interglacial periods (Holocene and stage 5.5). The magnitude and pattern of changes are comparable in the Vostok ice core.

In this study, the geographical origin of ice core dust (ICD) in cold periods has been investigated at both sites through $^{87}Sr/^{86}Sr$ versus $^{143}Nd/^{144}Nd$ isotopic tracers, following the previous studies of Grousset et al. [Earth Planet. Sci. Lett. 111 (1992) 175] and Basile et al. [Earth Planet. Sci. Lett. 146 (1997) 573].

The new data and the existing ones allow to define the isotopic fields for dust at the two Antarctic sites that are almost identical and restricted into the $0.708 < {}^{87}Sr/{}^{86}Sr < 0.711$ and $-5 < \varepsilon_{Nd}(0) < +5$ ranges. This suggests a common geographical provenance for dust at Vostok and Dome C and for all the glacial periods of the late Pleistocene.

To decipher the ICD provenance, more than 50 samples of loess and aeolian deposits, sands and fluvioglacial sediments from the Potential Source Areas (PSAs) of the Southern Hemisphere have been collected. However, the methodology has been

* Corresponding author. Laboratoire de Glaciologie et de Géophysique de l'Environnement, 54, rue Moliere, BP96, F-38402, Saint Martin d'Hères, France. Tel.: +33-476-824244; fax: +33-476-824201.

E-mail addresses: bdelmonte@nest.it (B. Delmonte), Isabelle.Basile@univ-reunion.fr (I. Basile-Doelsch), petit@glaciog.ujf-grenoble.fr (J.-R. Petit), valter.maggi@unimib.it (V. Maggi), Marie.Revel@ujf-grenoble.fr (M. Revel-Rolland), jagoutz@mailserver.mpch-mainz.mpg.de (E. Jagoutz), grousset@epoc.u-bordeaux.fr (F. Grousset).

0012-8252/$ - see front matter
doi:10.1016/j.earscirev.2003.10.004

refined with respect to former studies. First, the isotopic fractionation that can occur in function of grain size has been taken into account, and the PSA's signature has been defined in the <5 μm size range, within which fine-grained dust reaching Antarctica is found. Moreover, a possible contribution from carbonates on the samples from PSAs has also been also considered.

South Africa and Australia can be excluded as dominant sources, but a partial overlap arises among southern South America, New Zealand and the Antarctic Dry Valleys isotopic fields, these latter two documented for the first time.

A possible contribution from all these three sources cannot be excluded, but complementary arguments suggest the dominant contribution to East Antarctic dust in glacial times deriving from the southern South American region of Patagonia and the Pampas.

This study shows a first-order uniformity in the dust flux and geographical provenance to the East Antarctica plateau during glacial periods.

Keywords: Dust; Ice cores; Antarctica; Sr–Nd; Paleoclimate

1. Introduction

Windblown mineral aerosol (dust) could play an important role in the climate system; however, there are still considerable uncertainties in the quantitative estimation of direct (e.g., scattering and absorption of thermal radiation) and indirect effects of dust on the global energy balance, both in magnitude and sign (IPCC, 2001).

Mineral dust has also an important role on terrestrial (e.g., Swap et al., 1992) and marine (e.g., Hutchins and Brunland, 1998) ecosystems by providing nutrients, like some trace metals representing the limiting factor for some marine biological communities (e.g., Fung et al., 2000). The dust input can potentially influence the global carbon cycle and the atmospheric greenhouse gas content, but the magnitude of such a possible impact of dust is still highly uncertain.

The conscience of the importance of mineral aerosol on climate has led to substantial improvements in the study of physical and radiative characteristics of dust and in dust-cycle models, in order to simulate and predict in a reliable way the dust impacts on climate. However, the scarcity of global data sets determining model input parameters and validating model results makes the simulation of the global dust cycle still uncertain. Published data on global dust emission estimations for present time, for example, span a very large range, from about 100 Mtons $year^{-1}$ to about 3000 or even 5000 Mtons $year^{-1}$ (IPCC, 2001), and about 800–1700 Mtons $year^{-1}$ according to one of the most recent global dust models (Tegen et al., 2002a). Observations around the globe are very scarce, and they are often representative of a limited period of time; local observations are frequently extrapolated to yield a global estimate even if they come from specific regions having conditions that are not necessarily typical of all dust-source regions. Moreover, there are many desert areas in the world that are still too poorly sampled (Tegen et al., 2002b).

The prediction of the impact of changing mineral aerosol loading on future climates necessitates that earth system models could reproduce the (first-order) pattern of dust transport and deposition under modern climate and under different climatic conditions, like those that occurred in the past. The natural archives of paleoclimatic history like marine sediments, terrestrial deposits and ice cores are very precious in this respect since they give evidence and allow to quantify the huge variations in atmospheric dust load in association with the major climatic changes during the Quaternary. The numerous archives for paleo-dust cycle assembled in the DIRTMAP database (Kohfeld and Harrison, 2001) evidence that variations in dustiness were neither uniform nor ubiquitous all over the globe (Mahowald et al., 1999).

Polar ice cores archive mineral aerosol exclusively of aeolian origin, windblown long distance from the continents. The Vostok (East Antarctica, 78°28′ S, 106°48′ E) ice core, keeping the memory of 420,000 years of climatic and atmospheric history, revealed that the dust input to Antarctica was maximum during pleniglacial periods, lower during stadials and interstadials, and minimum in interglacials (Petit et al., 1999).

One of the first East Antarctic ice cores was recovered at the site of Dome C (74°39′ S, 124°10′ E) in

1978, and we will refer to this as the *old* Dome C core (Lorius et al., 1979). About 80 km from this site, a new ice core has been obtained in recent years in the framework of the *European Project for Ice Coring in Antarctica* (EPICA-Dome C ice core 75°06′ S, 123°21′ E). The first 580 m of this core (called *EDC1*) provided a new dust record at high time resolution for the last 27,000 years (Delmonte et al., 2002). Today, the availability of the 2200 m deep EPICA-Dome C (*EDC2*) ice core allows to extend the climatic sequence to the last ~220,000 years. The new dust record is presented in this work and compared with that from Vostok, located ca. 550 km apart.

The objective of this work is the documentation of the dust cycle towards the East Antarctic plateau in glacial periods. In particular, we will compare EPICA and Vostok records in order to document the flux and the geographical provenance variability at the scale of Eastern Antarctica. For this latter purpose, we followed a geochemical approach introduced by Grousset et al. (1992) and developed by Basile et al. (1997). The $^{87}Sr/^{86}Sr$ versus $^{143}Nd/^{144}Nd$ isotopic ratios are used as tracers for dust provenance and the ice core dust (ICD) signature is compared with that of the Potential Source Areas (PSAs) of the Southern Hemisphere. Many new samples have been collected through the help of several colleagues around the world, in order to document as completely as possible the possible sources for dust in East Antarctica.

In this study, however, the source identification method has been substantially improved with respect to previous studies; since the ICD is fine-grained (<5 μm), its signature is systematically compared to that of PSAs in the equivalent size range because isotopic fractionation can occur in function of particle size (e.g., Basile et al., 1997; Smith et al., 2003). Also, some leaching tests have been performed on some PSA samples in order to remove the eventual contribution from carbonates, that can potentially alter the original isotopic signature. Moreover, the ICD samples have been extracted from EPICA and Vostok ice cores by centrifugation, in order to prevent contribution from marine Sr. The new data, added with the existing ones, provide an exhaustive documentation of the isotopic signature of dust reaching the East Antarctic plateau in glacial periods.

2. Samples and analytical methods

2.1. Sampling the ice core dust

2.1.1. Samples for concentration measurements

A first set of samples for dust concentration measurements have been selected from the EPICA-EDC1 ice core every 120–140 cm from 100 to 780 m, for a total of about 550 samples. The sampling resolution is about one sample per 50 years from 100 to 480 m (2–18 kyears BP, according to Schwander et al., 2001) and one sample per 100–120 years from 480 to 780 m (18–45 kyears BP). From 780 to 2200 m, other 260 samples were regularly selected from the EPICA-EDC2 ice core every 550 cm of depth (corresponding to one sample per 700 years on average). For all the profile, each sample (5–6 cm) is representative of ca. 3 years of accumulation.

The average resolution of the dust concentration profile from Vostok ice core (Petit et al., 1999) is about one sample per 7 m, i.e., one sample per ca. 600 years.

2.1.2. Samples for isotopic measurements

2.1.2.1. Ice core dust extraction. On the basis of the dust concentration profiles (Fig. 1), we selected two samples for each glacial stage (2, 4 and 6) from EPICA ice core (see Table 1a for depths and ages) and two samples from the Vostok ice core (stage 6, Table 1a) for isotopic composition measurements. For this latter ice core, Sr–Nd isotopic measurements were already performed by Basile et al. (1997) on dust from glacial stages 4, 6, 8, 10 and 12.

The selected pieces of ice have been decontaminated by three repeated washings in ultra-pure water (MilliQ), in a class 100 clean room (LGGE-CNRS, Grenoble). Because of possible Sr contamination due to marine aerosols, the method by evaporation of melted ice used in Grousset et al. (1992) and Basile et al. (1997) was avoided. The mineral fraction was extracted by centrifugation from an initial sample of 300–900 g in weight, removing the supernate liquid through a syringe and evaporating the final remaining water (~20–30 ml).

The average mass of the sample, estimated by Coulter Counter, spanned from 50 to 150 μg of dust, corresponding to ~20–50 ng of total Sr and ~1–4 ng of total Nd, assuming an average upper continental

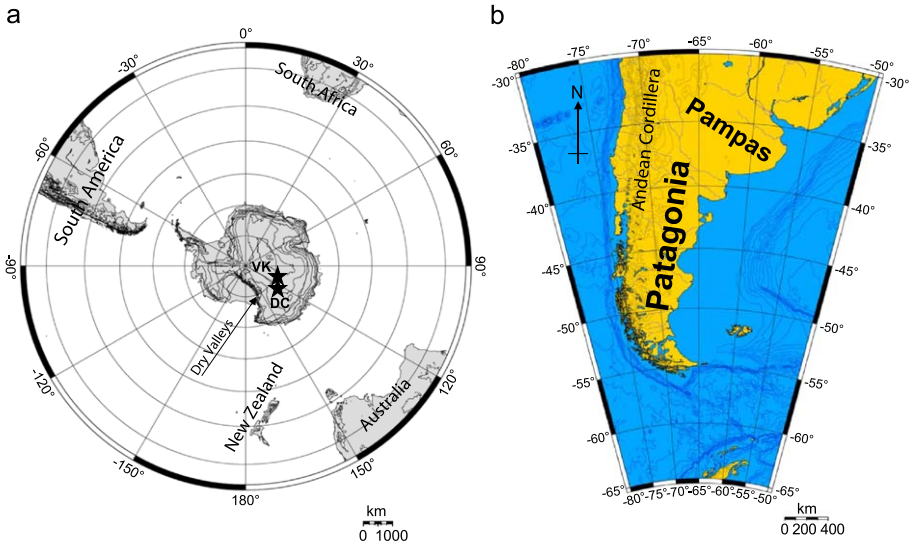

Fig. 1. Geographic maps. (a) Location of the potential sources for dust in the Southern Hemisphere, and of the two East Antarctic sites of Dome C (DC) and Vostok (VK). (b) South American regions discussed in the text.

crust (UCC) concentration for both elements of 350 and 26 ppm, respectively (Taylor and McLennan, 1985).

The dust from EPICA-Dome C sample at 570 m has been split into two aliquots that have been subjected to distinct chemistry treatments, and Sr isotopic composition has been measured from both aliquots to check the reproducibility of the analysis. Since the amount of Nd from that sample was already very low, an analogue test on this element could not be performed.

Coulter Counter analysis of the supernate evidenced that it still contained some very diluted particles even after centrifugation, whose size distribution was the same as for the total initial sample. To check for eventual mineralogical and hence isotopic differentiation, the isotopic composition of dust from the two Vostok samples analysed in this work (see Table 1a) has been measured both for the centrifuged (bottom) samples and for the filtered supernate (filter porosity 0.4 μm).

2.1.2.2. Sr and Nd extraction from ice core dust. The dissolution and all other chemical procedures on ICD samples have been carried out under clean laboratory conditions at the Department of Cosmochemistry of the Max Plank Institute (MPI) in Mainz (Germany). Dissolution was made in hermetically closed Teflon beakers in a mixture of concentrated [$HF + HClO_4$] on a hot plate. Then, separations of Sr and Nd have been made through liquid ionic chromatographic columns (primary and secondary columns).

Primary columns were made from pure quartz and filled with ca. 4 cm^3 of Bio-Rad 50W-x8 resin, after careful cleaning. After each passage of sample through primary columns these were cleaned with concentrated HCl and backwashed before use. For isolation of Nd, reverse phase chromatography has been used. The rare earth elements (REEs) were loaded into secondary columns (Micro-columns) also made from pure quartz and filled with Teflon-powder as inert phase, coated with an ion-exchanger (HDEHP). As for primary columns, also secondary columns were washed with strong HCl after each passage of sample. Each sample has been processed twice to improve purification. All acids and water used were specially cleaned. Deionised water was thrice distilled in a quartz distiller with the last step subboiling and acids were distilled twice by subboiling. This, among other things, allows to reduce procedural blanks, that were around 0.04–0.09% and 0.4–1.1% for Sr and Nd sample weights, respectively.

2.2. Samples from PSAs

2.2.1. What is a PSA sample?

A PSA sample can be either (1) a primary source of mineral aerosol, derived directly from the mechanical

and/or chemical alteration of the parent material (e.g., moraines) or (2) a secondary source for dust, that is a mixture of particles already subjected to a phase of aeolian (e.g., loess and loess-like deposits) and/or liquid (e.g., fluvioglacial sediments) transport. In any case, the dust deposit from which a PSA sample has been collected should be—or should have been in the past—an active source for dust. Areas where the recent geomorphological history has allowed concentration of fine-grained material, like paleolake beds, glacial outwash plains, riverine floodplains and alluvial fans, are powerful dust sources (Tegen et al., 2002a). Recent TOMS satellite observations (Prospero et al., 2002) have shown that sands and sand dune systems are not good sources for long range transports of dust in general, since they are devoid of the fine fraction and contain larger particles with very high settling velocity.

Climatic conditions influence greatly the dust source strength: Weak sources at present time could have been very important in the past and vice versa. It is the case, for instance, of the thick loess deposits now buried under vegetated soils that are common for example in the argentine plains east of the Andean cordillera. Beside pedogenesis and vegetation cover, other factors potentially reducing the strength of a source are the lack of renewal of small particles, surface crusting, soil moisture and surface roughness (Tegen et al., 2002b).

2.2.2. Samples collected for this study

A total of more than 55 samples from the South Hemisphere continents (Fig. 1a) have been collected; in particular, southern South America (south of 31°S, Fig. 1b) has been documented in detail through 24 samples from the Pampas, Patagonia and Chile, and for the first time also New Zealand (15 samples) and the Antarctic Dry Valleys (9 samples).

About 2% of Antarctica is ice free, for a total area equivalent to the size of New Zealand. These areas occur as isolated patches of rocks around the coast in East Antarctica, in the Transantarctic Mountains, crossing the Continent from Cape Adare to the Shackleton Mountains, and in the Antarctic Peninsula, where rocks are younger and similar to the Andes of South America (Campbell and Claridge, 1987). Antarctic samples from the McMurdo Dry Valleys are considered as a separate group; this region occupies the southern portion of the Victoria Land and the Scott Coast, and is roughly defined as extending from 76°30′ S to 78°30′ S, and from 160°00′ E to 164°30′ E (USGS National Mapping Information System).

Australia did not appear as dominant source in glacial periods according to previous studies (Basile et al., 1997), and only two samples from this region have been collected; one of them represents a huge sand storm that reached the area of Canberra on 16th October 2002.

Samples mainly consist of loess and loess-like deposits, silts and sands, fluvioglacial sediments, aeolian deposits and moraines. Only three samples consist of soils. The nature, geographical location and (if known) age of each is reported in Table 1b. Theoretically, ICD should be compared to a contemporaneous PSA sample, but it can be assumed that for the short geological time period investigated (late Quaternary), the Sr and Nd isotopic signatures of the sources are constant.

We did not consider other big dust sources from the Northern Hemisphere like the Sahara and the Arabian Peninsula, since tropospheric impurities are removed through the rain bands of the Intertropical Convergence Zone (Andersen, 1998), and the cross-equatorial dust transport is very reduced (Lunt and Valdes, 2002).

2.2.3. Sample treatment

2.2.3.1. Size selection. All PSA samples have been selected for their <5 μm fraction according to the following procedure. MilliQ water was added to the bulk PSA samples to obtain a particle suspension, which was submitted to sonification for about 10 min for aggregate dispersion. The fine fraction has been isolated from the bulk according to the Stoke's law through humid sedimentation, and separated using a syringe. The size of the particles collected was carefully checked with a Laser Particle Counter, and only samples presenting at least 95% of the total mass (>99.8% of total number) finer than 5 μm have been accepted. The mass size distributions of PSA samples appeared log-normally distributed and very similar to that of ice core dust samples (see the examples reported in Delmonte et al., 2002), despite the two different techniques adopted for measurements (Coul-

Table 1
Data from ICD and PSA samples
(a)

Ice core dust sample (depth)	Data source	Age (eventual)	Geographic coordinates	$^{87}Sr/^{86}Sr$	$^{143}Nd/^{144}Nd$	$\varepsilon_{Nd}(0)$
Dome C						
EPICA Dome C (518–520 m)	[1]	Stage 2 (21–22 kyears BP)	75°06′ S, 123°24′ E	0.708595 (21)	0.512553 (27)	−1.66
EPICA Dome C (570 m)	[1]	Stage 2 (26.4 kyears BP)	75°06′ S, 123°24′ E	0.708834 (37)	0.512512 (32)	−2.46
EPICA Dome C (570 m)-repeated	[1]	Stage 2 (26.4 kyears BP)	75°06′ S, 123°24′ E	0.709033 (81)		
EPICA Dome C (957–963 m)	[1]	Stage 4 (about 60 kyears BP)	75°06′ S, 123°24′ E	0.708443 (19)	0.512602 (75)	−0.70
EPICA Dome C (996 m)	[1]	Stage 4 (about 60 kyears BP)	75°06′ S, 123°24′ E	0.708803 (20)	0.512538 (26)	−1.95
EPICA Dome C (around 1790 m)	[1]	Stage 6 (around 150 kyears BP)	75°06′ S, 123°24′ E	0.708897 (20)	0.512564 (28)	−1.44
EPICA Dome C (between 1880–1890 m)	[1]	Stage 6 (around 150 kyears BP)	75°06′ S, 123°24′ E	0.709537 (17)	0.512683 (16)	0.88
Old Dome C (550–589 m)	[4]	Stage 2 (16–18 kyears BP)	74°39′ S, 124°10′ E	0.708707 (60)	0.512894 (39)	4.99
Old Dome C (516 m)	[3]	Stage 2 (15.9 kyears BP)	74°39′ S, 124°10′ E	0.708753 (56)	0.512484 (32)	−3.00
Vostok						
Vostok (2107 m)-F	[1]	Stage 6 (around 150 kyears BP)	78°28′ S, 106°48′ E	0.708818 (19)	0.512555 (52)	−1.62
Vostok (2107 m)	[1]	Stage 6 (around 150 kyears BP)	78°28′ S, 106°48′ E	0.708220 (15)	0.512628 (28)	−0.20
Vostok (2054 m)-F-I	[1]	Stage 6 (around 150 kyears BP)	78°28′ S, 106°48′ E	0.711035 (38)	0.512445 (52)	−3.76
Vostok (2054 m)-F-II	[1]	Stage 6 (around 150 kyears BP)	78°28′ S, 106°48′ E	0.711254 (91)		
Vostok (2054 m)	[1]	Stage 6 (around 150 kyears BP)	78°28′ S, 106°48′ E	0.709579 (17)		
Vostok (1965 m)	[3]	Stage 6 (around 150 kyears BP)	78°28′ S, 106°48′ E	0.709468 (32)	0.512545 (14)	−1.81
Vostok (2873 m)	[3]	Stage 8 (around 268 kyears BP)	78°28′ S, 106°48′ E	0.711129 (33)	0.512393 (48)	−4.78
Vostok (3144 m)	[3]	Stage 10 (around 340 kyears BP)	78°28′ S, 106°48′ E	0.708460 (36)	0.512530 (27)	−2.11
Vostok (3347 m)	[3]	Stage 12 (around 421 kyears BP)	78°28′ S, 106°48′ E	0.710846 (46)	0.512481 (12)	−3.06
Vostok (905–911 m)	[2]	Stage 4 (60.4–60.9 kyears)	78°28′ S, 106°48′ E	0.708047 (09)	0.512694 (28)	1.09
Vostok (911–919 m)	[2]	Stage 4 (60.9–61.7 kyears)	78°28′ S, 106°48′ E	0.708404 (12)		
Vostok (2106–2133 m)	[2]	Stade 6 (158.8–162.6 kyears)	78°28′ S, 106°48′ E	0.708219 (11)	0.512836 (40)	3.86
Vostok (2134–2169 m)	[2]	Stade 6 (162.7–166.8 kyears)	78°28′ S, 106°48′ E	0.708452 (12)	0.512710 (121)	1.40

Table 1 (*continued*)
(b)

Code	Geographical region	Size	Data source	Kind of sample	Age (eventual)	Geographic coordinates	$^{87}Sr/^{86}Sr$ ($\pm 2\sigma \times 10^{-6}$)	$^{143}Nd/^{144}Nd$ ($\pm 2\sigma \times 10^{-6}$)	$\varepsilon_{Nd}(0)$
South Africa									
SAFR1	Namibia—Sesriem, dune	< 5 μm	[1]	S		24°29′ S, 15°48′ E	0.721330 (117)	0.512098 (27)	− 10.53
SAFR2	Namibia—Sossusvlei	< 5 μm	[1]	S		24°42′ S, 15°17′ E	0.721042 (21)	0.512083 (09)	− 10.83
SAFR3	Namibia—Kuiseb River, intermittent stream	< 5 μm	[1]	S		23°07′ S, 14°30′ E	0.722849 (19)	0.512104 (19)	− 10.42
SAFR4	Namibia—Sossusvlei, dune	< 5 μm	[1]	S		24°42′ S, 15°17′ E	0.719708 (23)	0.512207 (20)	− 8.41
SAFR5	Kalahari Desert	< 5 μm	[4]	L		27°S, 20°E	0.747157 (33)	0.511382 (22)	− 24.50
SAFR6	Windblown dust from transect Port Elisabeth-Cape Town	< 5 μm	[1]	Ap		34°42′ S, 26°32′ E to 33°55′ S, 18°25′ E	0.724163 (18)	0.512100 (14)	− 10.49
South America									
SA1	Puerto Madryn	< 5 μm	[1]	Ad	Pleistocene–Holocene	42°46′ S, 65°03′ W	0.707320 (23)	0.512644 (09)	0.12
SA2	Pampas 1	< 5 μm	[1]	Ad	20–25 kyears BP	37°57′ S, 57°38′ W	0.708547 (19)	0.512628 (11)	− 0.20
SA3	Pampas 2	< 5 μm	[1]	Ad	20–25 kyears BP	34°54′ S, 58°01′ W (*)	0.710311 (16)	0.512524 (15)	− 2.22
SA4	Pampas 3	< 5 μm	[1]	Ad	< 23 kyears BP	25 km NW from (*)	0.709908 (21)	0.512541 (11)	− 1.89
SA5	Pampas 4	< 5 μm	[1]	Fd	about 20 kyears BP	33°49′ S, 59°31′ W	0.711218 (26)	0.512496 (14)	− 2.77
SA6	Cordoba area	< 5 μm	[1]	L	10–20 kyears B.P	31°39′ S, 64°08′ W	0.709357 (22)	0.512483 (08)	− 3.02
SA7	Argentina—S. Carlos de Bariloche	< 5 μm	[1]	slt-LL		41°09′ S, 71°18′ W	0.704604 (18)	0.512777 (09)	2.71
SA8	Isla Grande de Chiloe—I	< 5 μm	[1]	fS	Holocene	48°38′ S, 74°06′ W	0.707207 (20)	0.512709 (17)	1.38
SA9	Isla Grande de Chiloe—II	< 5 μm	[1]	S	Holocene	48°38′ S, 74°06′ W	0.706891 (16)	0.512726 (12)	1.72
SA10	Isla Grande de Chiloe—III	< 5 μm	[1]	Ad	modern	48°38′ S, 74°06′ W	0.70715 (24)	0.512597 (29)	− 0.80
SA11	Torres del Paine N. Park—I	< 5 μm	[1]	S (M)		51°04′ S, 73°09′ W	0.707298 (19)	0.512489 (15)	− 2.91
SA12	Torres del Paine N. Park—II	< 5 μm	[1]	S (M)	Pre-Holocene	51°04′ S, 73°09′ W	0.70862 (14)	0.512552 (14)	− 1.68
SA13	Punta Arenas—I	< 5 μm	[1]	slt		53°09′ S, 70°55′ W	0.70988 (19)	0.512569 (08)	− 1.35
SA14	Tierra del Fuego	< 5 μm	[1]	slt		53°18′ S, 70°22′ W	0.711806 (21)	0.512439 (07)	− 3.88
SA15	Punta Arenas—II	< 5 μm	[1]	slt-LL		53°09′ S, 70°55′ W	0.705364 (21)	0.512743 (10)	2.05
SA16	Aeolian dust event—Buenos Aires (28–08–1997)	< 5 μm	[1]	Ap		34°35′ S, 58°40′ W	0.713088 (28)	0.512227 (08)	− 8.02

(continued on next page)

Table 1 (*continued*)
(b)

Code	Geographical region	Size	Data source	Kind of sample	Age (eventual)	Geographic coordinates	$^{87}Sr/^{86}Sr$ ($\pm 2\sigma \times 10^{-6}$)	$^{143}Nd/^{144}Nd$ ($\pm 2\sigma \times 10^{-6}$)	$\varepsilon_{Nd}(0)$
South America									
SA17	Coihaique region—I	< 5 μm	[1]			45°34′ S, 72°04′ W	0.712930 (10)	0.512528 (16)	− 2.15
SA18	Coihaique region—II	< 5 μm	[1]			45°34′ S, 72°04′ W	0.705377 (08)	0.512655 (22)	0.33
SA19	Coihaique region—III	< 5 μm	[1]			45°34′ S, 72°04′ W	0.704597 (37)	0.512659 (11)	0.41
SA20	South America (##)—I	< 5 μm	[1]				0.706852 (10)	0.512640 (15)	0.04
SA21	South America (##)—II	< 5 μm	[1]				0.711385 (09)	0.512368 (08)	− 5.27
SA22	South America (##)—III	< 5 μm	[1]				0.705507 (12)	0.512749 (14)	2.17
SA23	South America (##)—IV	< 5 μm	[1]				0.709443 (12)	0.512182 (16)	− 8.90
SA24	South America (##)—V	< 5 μm	[1]				0.704290 (28)	0.512686 (03)	0.94
SA25	Argentina	< 5 μm	[4]			38°S, 59°W	0.708749 (28)	0.513064 (17)	8.31
New Zealand									
NZ1	Southland—Te Anau	< 5 μm	[1]			45°24′ S, 167°42′ E	0.705183 (24)	0.512576 (11)	− 1.21
NZ2	Otago	< 5 μm	[1]	Fd		44°38′ S, 168°59′ E	0.709683 (19)	0.512442 (20)	− 3.82
NZ3	Raikaia river mouth	< 5 μm	[1]	Fd		43°44′ S, 172°02′ E	0.713883 (21)	0.512313 (10)	− 6.34
NZ4	South Island—ChC area	< 5 μm	[1]	slt-LL		43°28′ S, 172°31′ E	0.723239 (24)	0.512298 (20)	− 6.63
NZ5	Arthur's Pass	< 5 μm	[1]			43°17′ S, 171°42′ E	0.711657 (17)	0.512302 (12)	− 6.55
NZ6	Otago district	< 5 μm	[1]	Ad		44°48′ S, 169°20′ E	0.711190 (26)	0.512306 (17)	− 6.49
NZ7	Carterbury plains	< 5 μm	[1]	Loess		44°18′ S, 171°15′ E	0.710064 (27)	0.512404 (75)	− 4.56
NZ8	Dart Valley Moraine—Bottom valley	< 5 μm	[1]	M		44°S, 168°E	0.713591 (04)	0.512336 (05)	− 5.89
NZ9	Dart Valley Moraine—High valley	< 5 μm	[1]	M-1		44°S, 168°E	0.714148 (06)	0.512370 (03)	− 5.23
NZ10	Dart Valley Moraine—High valley	< 5 μm	[1]	M-2		44°S, 168°E	0.713260 (21)	0.512269 (158)	− 7.20
NZ11	N.Island: North Crater—Rotopaunga	< 5 μm	[1]	S		39°S, 175°E	0.705305 (11)	0.512635 (05)	− 0.06
NZ12	N.Island: South Crater—Mt. Tongariro	< 5 μm	[1]	S		39°S, 175°E	0.705449 (10)	0.512621 (04)	− 0.33
NZ13	N.Island: Wellington district	< 5 μm	[1]	Fd		39°S, 175°E	0.706065 (07)	0.512513 (24)	− 2.44
NZ14	N.Island: Red Crater	< 5 μm	[1]			39°S, 175°E	0.705012 (13)	0.512633 (11)	− 0.10
NZ15	Tongarino Park	< 5 μm	[1]	S		39°S, 175°E	0.705354 (07)	0.512580 (24)	− 1.13

Table 1 (*continued*)
(b)

Code	Geographical region	Size	Data source	Kind of sample	Age (eventual)	Geographic coordinates	$^{87}Sr/^{86}Sr$ ($\pm 2\sigma \times 10^{-6}$)	$^{143}Nd/^{144}Nd$ ($\pm 2\sigma \times 10^{-6}$)	$\varepsilon_{Nd}(0)$
Antarctic Dry Valleys									
A1	Pearse Valley	< 5 μm	[1]	S		77°43′ S, 161°23′ E	0.713913 (10)	0.511997 (08)	− 12.50
A2	Pat's peak ridge—Cape Crozier	< 5 μm	[1]	S		77°31′ S, 169°24′ E	0.703194 (15)	0.512929 (07)	5.68
A3	Hanson Ridge	< 5 μm	[1]			77°17′ S, 163°15′ E	0.709797 (41)	0.512492 (08)	− 2.85
A4	Hanson Ridge	< 5 μm	[1]			77°17′ S, 163°15′ E	0.710038 (23)	0.512585 (11)	− 1.03
A5	McMurdo—I	< 5 μm	[1]	S		77°30′ S, 165°E	0.703357 (09)	0.512818 (08)	3.51
A6	McMurdo—II	< 5 μm	[1]	S		77°30′ S, 165°E	0.705804 (07)	0.512687 (02)	0.96
A7	Lake Hoare, Taylor Valley	< 5 μm	[1]			77°37′ S, 163°11′ E	0.711757 (31)	0.512306 (10)	− 6.48
A8	South Shore lake Fryxell	< 5 μm	[1]	S		77°38′ S, 162°51′ E	0.708914 (11)	0.512376 (12)	− 5.11
A9	Bull pass	< 5 μm	[1]	S			0.715600 (14)	0.512129 (19)	− 9.93
Antarctica									
A10	Northern Victoria Land (NVL), Terranova Bay	< 5 μm	[1]	S		74°50′ S, 164°30′ E	0.748814 (16)	0.511919 (09)	− 14.03
A11	Terre Adelie (Grousset et al., 1992)	< 5 μm	[4]	M		67°S, 139°E	0.774102 (33)	0.512117 (28)	− 10.16
Australia									
AUS1	Aeolian dust event, Canberra 16/10/02	10 μm	[1]	Ap			0,716736 (26)	0.512271 (10)	− 7.16
AUS2	Brown's Creek, Central Highlands, NSW	~ 10 μm	[1]	Soil			0,719663 (20)	0.512125 (08)	− 10.01
AUS3	Australia (Grousset et al., 1992)	< 5 μm	[4]				0.740074 (32)	0.512128 (26)	− 9.95

In (a), the ice core samples and the relative depths are reported, together with the source of data ([1] = this work; [2] = Basile et al., 1997; [3] = Basile, 1997; [4] = Grousset et al., 1992), the age of the sample, the location of the drilling site and the isotopic ratios. The Vostok samples marked with "F" (F-I and F-II) have been obtained through filtration of the centrifugation supernate. One EPICA-Dome C sample (570 m) was split in two aliquots and Sr has been measured from both.
In (b), data from PSA samples (fraction < 5 μm) are reported. From left to right: the code and the geographical provenance region for each sample, the source of the data (see (a)), the kind of sample (L = loess; Ad = Aeolian deposit; Ap = present-day Aeolian dust; S = sand; fS = fine sand; M = moraine; Fd = fluvioglacial deposit; slt = silt; s = soil; extension-LL = loess-like; ICD = ice core dust), the age of the deposit when available, the geographical coordinates of the site, the $^{87}Sr/^{86}Sr$ ratio, the $^{143}Nd/^{144}Nd$ ($\pm 2\sigma \times 10^{-6}$ in brackets) and $\varepsilon_{Nd}(0)$.

ter Counter and Laser). The liquid suspension of < 5 μm particles (~ 30 ml) has been frozen and lyophilised. The mass of each sample spanned between 5 and 50 mg. Only the two Australian samples have not been selected in size; for them, the mass size distribution measured by Coulter Counter evidenced a mass modal diameter of ~ 10 μm.

2.2.3.2. Leaching procedure. Fifteen samples already selected for their < 5μm fraction have been split

in two aliquots, one of which has been leached by adding acetic acid buffered at pH 5 at room temperature. After 30–40 min, the particles have been recuperated by centrifugation, and subsequently re-washed three times in MilliQ water and again recuperated through centrifugation cycles. This procedure is supposed to remove calcite from the samples and was used for example by Biscaye et al. (1997). The average weights of the dry samples range from ~ 5 to 10 mg.

The second aliquot has not been leached and was directly subjected to the chemical separation of the elements.

2.2.3.3. Sr and Nd extraction. The chemical treatment of PSA samples has been performed in the clean room in two sets: one set in EPOC laboratory (Bordeaux, France) and one in set in CEREGE laboratory (Aix en Provence, France), following the same procedure. The two samples from Australia have been treated in Canberra at the Research School of Earth Sciences (Australian National University, Canberra), following the same procedure.

Dissolution of dust has been made through a first acid attack with a mixture of [$HNO_3 + HF + HClO_4$], and a second with [$HNO_3 + HCl$] on hot plate. The Sr and Nd have been then extracted by single passage through primary and secondary ionic chromatographic columns. The total blanks of the whole procedure were about 0.03–0.06% and 0.07–0.15% of sample Sr and Nd total weights, respectively, and therefore can be considered negligible.

2.3. Dust concentration measurements

Dust concentration measurements from the first 2200 m of the EPICA-Dome C ice core have been performed using a particle counter (Coulter Counter Multisizer IIe©, 256 channels) set up in a class 100 clean room. The procedures for sample preparation and decontamination are described in Delmonte et al. (2002) and are the same as used by Petit et al. (1999) for the Vostok ice core which we use for comparison. Analyses on Vostok dust, however, were performed with a slightly different particle counter (TA-II) with lower particle-size resolution (16 channels instead of 256). Each concentration data is the average of three repeated analysis, and the mass of particles has been calculated from the volume assuming an average crustal density of 2.5 g/cm^3 and a spherical shape for particles.

2.4. Measurements of Sr and Nd isotopic ratios

The quantity of Sr and Nd extracted varies of a factor of 100 between the PSA samples and the ICD glacial samples. The average quantity of Sr and Nd from source samples is in the order of ~ 2600 and ~ 200 ng, respectively, while for ICD, they decrease to ~ 35 and ~ 2.5 ng. These differences and, in particular, the low amounts of Nd, justify the choice of two different Thermo-Ionisation Mass Sperctrometers (TIMS) for the analysis of the two groups of samples.

Isotopic measurements on ICD have been performed through a highly sensitive TIMS at the Department of Cosmochemistry of the Max Plank Institute of Mainz (Germany). The spectrometer was especially modified on the basis of Finnigan MAT261, in order to perform precise measurements of small samples (e.g., Bogdanovski, 1997). The high sensitivity of this mass spectrometer is provided by modifications to the ionization system, the vacuum and the registration systems, detailed in Bogdanovski (1997). It is well known that isotope analysis of Nd using NdO^+ ion beam is much more sensitive than using Nd^+ ion beam. Therefore, an inlet of pure oxygen into the source area was applied for measurements of this element.

Each Sr and Nd ratio represents the average of 600 individual ratios (120 blocks of 5 scans) obtained over 17–24 h for each sample. Measured La Jolla Standard $^{143}Nd/^{144}Nd$ and E and A Standard $^{87}Sr/^{86}Sr$ yielded 0.511859 ($\pm 20\ 10^{-6}$) and 0.710205 ($\pm 25\ 10^{-6}$), respectively, and for the accuracy required in this study, the results did not need to be normalized with respect to certified values of 0.511861 and 0.710409.

Isotopic measurements on all the PSA samples have been made using a TIMS Finnigan© MAT262 at CEREGE Laboratory (Aix en Provence, France), except for the two Australian samples that have been analysed at the Australian National University in Canberra (Australia) using a Finnigan© MAT261 multicollector. Measured AMES Standard $^{143}Nd/^{144}Nd$ and NBS987 Standard $^{87}Sr/^{86}Sr$ yielded 0.511942 ($\pm 9\ 10^{-6}$) and 0.710227 ($\pm 25\ 10^{-6}$), respectively; as for ICD, the accuracy is sufficient to avoid data normalization with respect to certified values of 0.511962 and 0.710248.

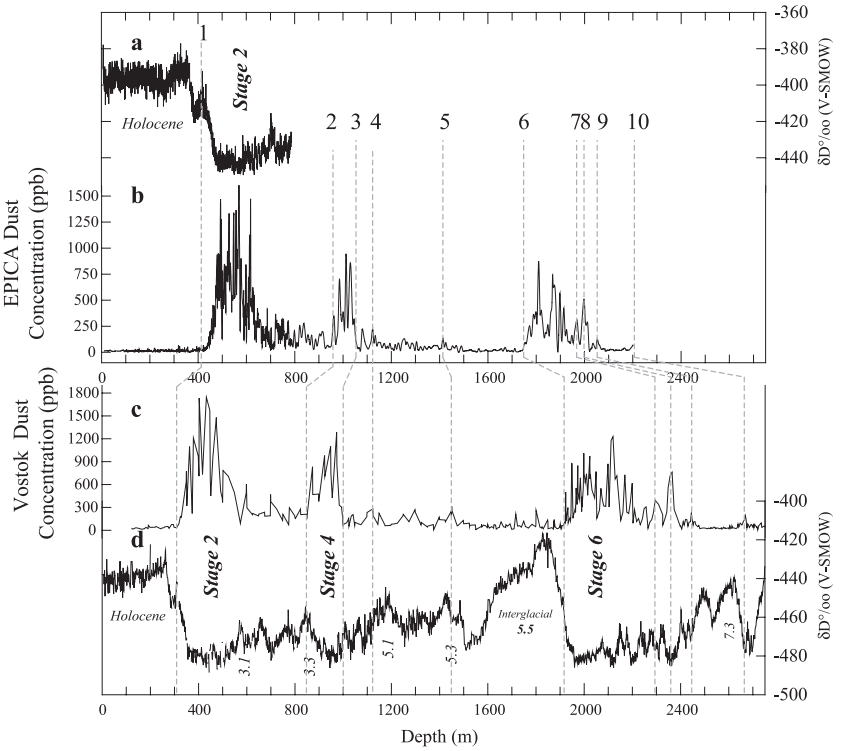

Fig. 2. Climate and dust records from EPICA-Dome C and Vostok ice cores. (a) EPICA deuterium record from Jouzel et al. (2001). (b) EPICA dust concentration record (ppb) until 2201 m depth. (c) Vostok dust concentration record (ppb), from Petit et al. (1999), until 2670 m. (d)Vostok deuterium record for the last ~ 220,000 years; the major climatic stages are indicated. The dashed lines linking EPICA and Vostok ice cores identify 10 common dust events, whose corresponding depths are reported in Table 2.

Neodymium ratios are defined as:

$$\varepsilon_{Nd}(0) = \frac{(^{143}Nd/^{144}Nd)_{meas}}{(^{143}Nd/^{144}Nd)_{CHUR}} - 1 \times 10^4$$

using the present-day chondritic uniform reservoir (CHUR) value for $^{143}Nd/^{144}Nd$ ratio of 0.512638 (Jacobsen and Wasserburg, 1980). The measured $^{143}Nd/^{144}Nd$ ratios have been corrected for mass fractionation by normalizing to $^{146}Nd/^{144}Nd = 0.7219$, while the $^{87}Sr/^{86}Sr$ ratios have been normalized to $^{86}Sr/^{88}Sr = 0.1194$.

3. Results

3.1. The EPICA dust concentration record

The EPICA isotopic record (proxy for temperature) is available from 0 to 780 m (Jouzel et al., 2001), and it is reported in Fig. 2a along with the dust profile obtained in this work for the first 2200 m of the core (Fig. 2b). Particles over all the profile presented a mean

Table 2
Depth of the 10 dust events marked in Fig. 2 allowing to link stratigraphically the EPICA and Vostok ice cores

Dust event	Event	Vostok depth (m)	EPICA depth (m)
1	End of stage 2	309	420
^{10}Be peak		610	742
2	End of stage 4	849	947
3	Beginning of stage 4	1000	1062
4		1123	1123
5		1450	1415
6	End of stage 6	1906	1744
7		2294	1970
8		2364	1997
9		2444	2052
10	End of stage 7.4	2670	2201

The depth of the ^{10}Be peak is also reported (Schwander et al., 2001).

diameter of ~ 2 μm, and any particle greater that ~ 5 μm has been found. From 0 down to 420 m, corresponding to the Holocene and the Antarctic Cold Reversal (ACR), the dust concentration is quite low, and during the Holocene, it is on average around 15 ppb (i.e., ~ 15 μg of dust per kilogram of ice). From 420 to 700 m, corresponding to glacial stage 2, dust concentrations are highly variable and can reach 1500 ppb; the average for the whole period is ~ 650 ppb. Between ~ 700 and ~ 950 m, ICD concentrations are still variable around ~ 150 ppb. Downward, a repeated similar pattern of high and variable levels of ICD

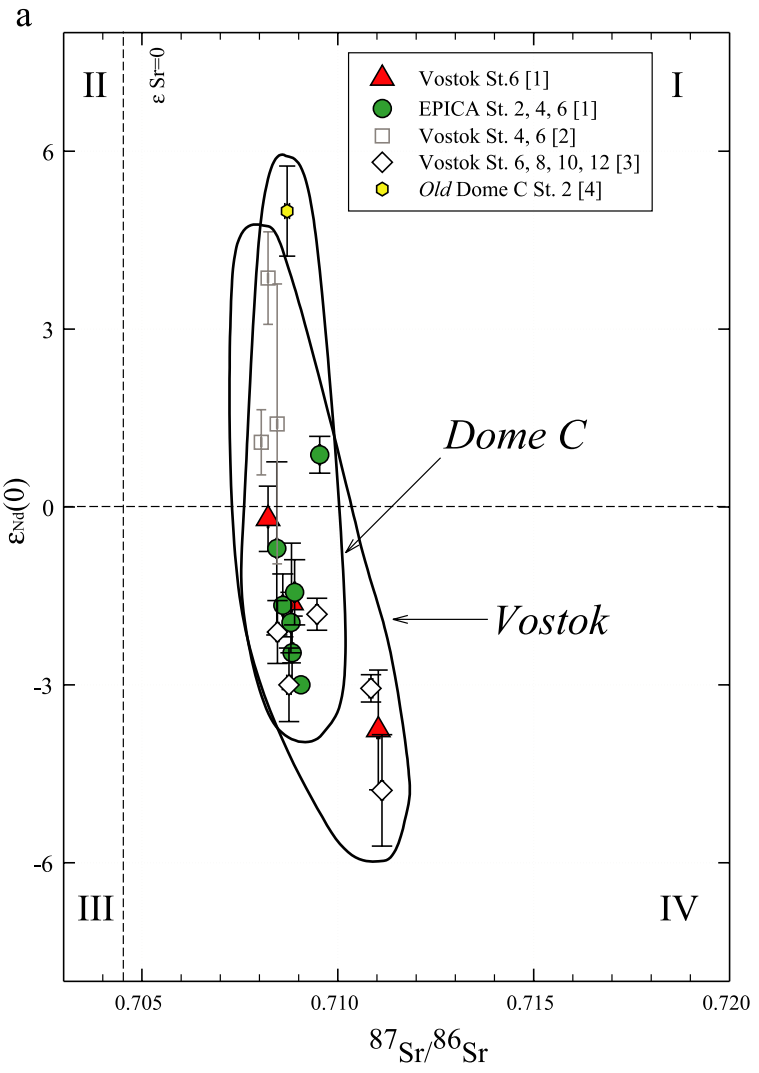

Fig. 3. $^{87}Sr/^{86}Sr$ versus $\varepsilon_{Nd}(0)$ plots. (a) Isotopic fields for Dome C and Vostok ice core dust with error bars (data from this work, Grousset et al., 1992; Basile et al., 1997; Basile, 1997). (b) Comparison between the ICD data and the signature of the <5 μm fraction of PSA samples. The four quadrants (I–IV) have been traced to facilitate the interpretation of the data by using the isotopic ratios of CHUR for Nd and UR (Uniform Reservoir) for Sr. The unfractionated mantle (Bulk Earth) $^{87}Sr/^{86}Sr$ was estimated 0.7045 by De Paolo and Wasserburg (1976) from the intersection of the chondritic ε_{Nd} line ($\varepsilon_{Nd}=0$) with the mantle Nd–Sr correlation line defined with Mid Ocean Ridge Basalts (MORBs). In this figure, the isotopic fields for South America, New Zealand, the Dry Valleys, South Africa and the ice core glacial dust have been arbitrarily defined on the basis of the available points. The Antarctic sample from Terre Adélie overpass the field spanned by the graph. Data and bibliographic source for each sample are reported in Table 1a,b.

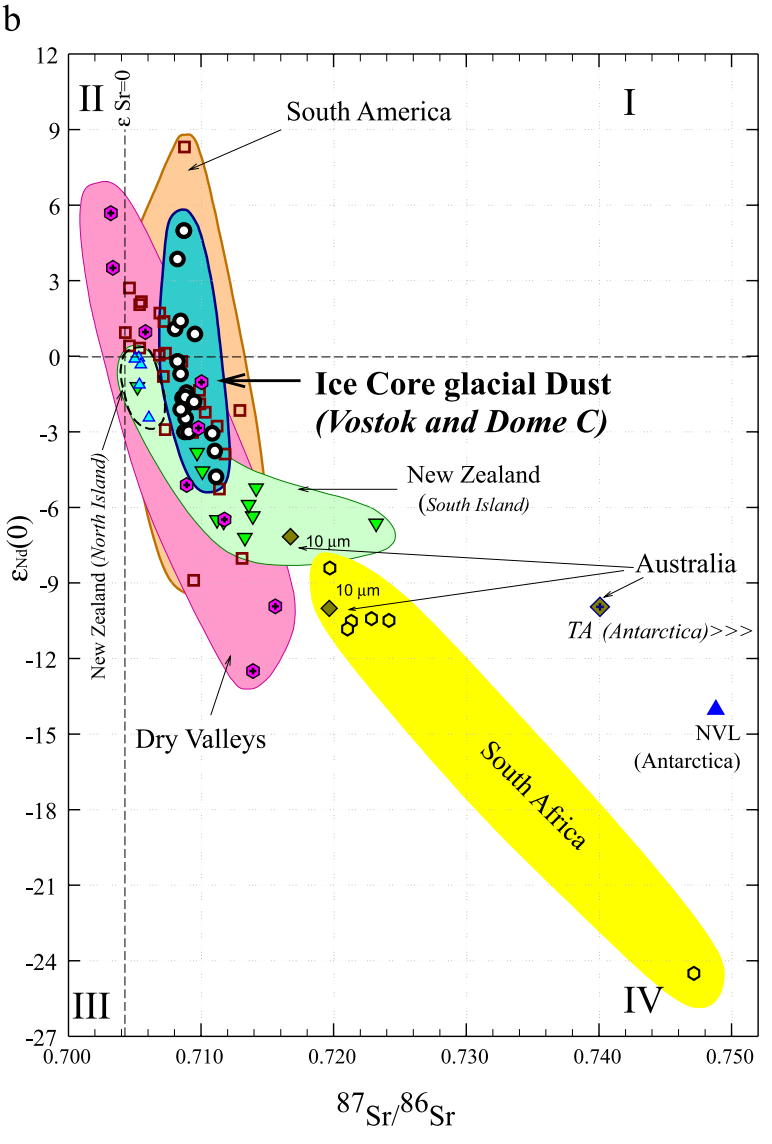

Fig. 3 (*continued*).

concentrations between 950 and 1060 m (~ 500 ppb) and between 1750 and 2050 m (~ 300 ppb), separated by low and almost constant levels of ICD concentrations (~ 45–50 ppb between 1060 and 1750 m and ~ 30–35 ppb between 2050 and 2200 m), can be observed.

The new EPICA dust record can be compared to the Vostok dust record (Fig. 2c,d from Petit et al., 1999). Despite the slightly different sampling resolution, the coherence of the two profiles is evident. The three big pulses observed in EPICA are also recorded in the Vostok ice core. These stratigraphical links allow to establish a depth-to-depth relationship and ultimately to have an estimation of the age through the deuterium profile of Vostok and the Vostok GT4 chronology.

In the EPICA core from 420 to 700 m, the ice corresponds to the cold stage 2 (~ 18–30 kyears BP),

from 950 to 1060 m, the ice corresponds to the cold stage 4 (~ 60–70 kyears BP), and from 1750 and 2050 m, the ice corresponds to the cold stage 6 (~ 135–165 kyears BP). On the opposite, periods with low concentrations correspond to interglacials and interstadials. Two interglacial periods are spanned by the EPICA record: the Holocene (first 350 m of ice), corresponding to the last 10 kyears, and the isotopic stage 5.5, which is the last interglacial (1550–1750 m), corresponding to the period from 120 to 130 kyears BP. The latter approximately corresponds to stage 5e of the Greenland GRIP ice core, and to the so-called Eemian interglacial in Europe.

The correlation can be refined through some well-isolated dust events recorded at both sites. In particular, 10 common events have been identified and are indicated in Fig. 2. Their respective depths are reported in Table 2 together with another marker corresponding to the depth of the ^{10}Be event (Schwander et al., 2001). The dust events correspond either to the end of periods characterized by a high dust concentrations (e.g., events 1, 2, 6 and 10 in Table 2) and well marked by the sharp fallout of dust, or to isolated dust events present in both records (e.g., events 4, 5, and 7–9 in Table 2). These correlations highlight that until ~ 1120 m, a common dust event is deeper in the EPICA than in the Vostok core, while the situation is reversed at higher depths; this because of differences in accumulation rate and glacier dynamics at the two sites. The dust event recorded in Vostok at about 2675 m (stage 7.4) does not seem to be reached in the EPICA core, whose deeper bottom sample analysed corresponds approximately the end of this event (220,000 years BP).

3.2. Isotopic signature of ice core glacial dust and source regions

The Sr–Nd isotopic ratios from EPICA and Vostok glacial samples measured in this work are reported in Table 1a and shown in Fig. 3a, along with previous results from Basile (1997), Basile et al. (1997) and Grousset et al. (1992) on the Vostok (stages 4, 6, 8, 10, 12) and on the old Dome C (stage 2) ice cores. It can be observed that the overall signature of the dust is restricted into the range of $0.708 < {}^{87}Sr/{}^{86}Sr < 0.711$ and $-5 < \varepsilon_{Nd}(0) < +5$. The isotopic fields of dust from the two ice cores overlap almost completely and we consider them to be identical. Strontium isotopes measured on two aliquots of the same samples (EPICA-570 m, Table 1a) show values of 0.708834 ($2\sigma = \pm 37 \times 10^{-6}$), and 0.709033 ($2\sigma = \pm 81 \times 10^{-6}$) and demonstrate that measurements are reproducible. The isotopic ratios of the centrifuged sample and the filtered supernate from one Vostok sample (Table 1a) show only slight differences, not significant with respect to the general interpretation of the results.

Isotopic signature of the different geographical source regions are reported in Table 1b and Fig. 3b. South Africa, Australia and East Antarctica (Terre Adelie and Northern Victoria Land NVL) evidence low radiogenic Nd (with $\varepsilon_{Nd}(0)$ values lower than −7) and high radiogenic Sr ($^{87}Sr/^{86}Sr > 0.717$). This signature is typical of crustal rocks (IVth quadrant, Fig. 3b), and is coherent at first approximation with the geological history of these continents. The Sr signature of the two Australian samples (10 μm in size) is expected to be rather less radiogenic than their fine (<5 μm) fraction, since smaller particles (clays) can bring more radiogenic $^{87}Sr/^{86}Sr$ (e.g., Biscaye and Dasch, 1971).

On the other hand, the signatures of New Zealand, the Dry Valleys of Antarctica and southern South America partly superpose one to the other (Fig. 3b). This could be anticipated by their similar tectonic context, since all three are young orogenic environments marked by andesitic volcanic activity. Similar characteristics can be found also in the Antarctic Peninsula, where exposed rocks are common (igneous intrusive rocks, volcanics and metamorphosed sediments), and that could be also considered as a potential dust source. From this area, we have no samples, but a geochemical similarity with the southern Andes of South America could be expected. (Campbell and Claridge, 1987).

The North Island of New Zealand, where five of our samples have been collected (NZ11 to NZ15, see dashed field in Fig. 3b), evidences a volcanic imprint, with $-2.4 < \varepsilon_{Nd}(0) < 0$ and $0.7050 < {}^{87}Sr/{}^{86}Sr < 0.7060$; this probably derives from the past volcanic activity of the Northland Volcanic Arc (until 15 Myears ago) and the Hauraki region (late Pleistocene)

and from the present volcanism in the Taupo Volcanic Zone. Rhyolites, andesites and dacites are common rocks in the North Island. Also in the Canterbury and Otago districts of the South Island, there are volcanic rocks (tholeiitic to alkaline basaltic rocks), heritage of Miocene and Pliocene intraplate volcanism, but overall, the volcanic imprint on sediments from South Island (samples NZ1 to NZ10) appears slightly less pronounced than in the North, and majority of the samples span the isotopic field between $0.709 < {}^{87}Sr/{}^{86}Sr < 0.723$ and $-3.8 < \varepsilon_{Nd}(0) < -7.2$ (with only one exception constituted by the sample NZ1 from Southland district).

The samples from the McMurdo Dry Valleys area include glacial sediments that are mixture of crustal and volcanic rocks keeping the imprint of the volcanism that began in the Late Miocene and continues to the present day. This justifies the wide $\varepsilon_{Nd}(0)$ interval spanned ($-12.5 < \varepsilon_{Nd}(0) < +5.7$). Strontium isotopes are relatively more restricted into the interval $0.703 < {}^{87}Sr/{}^{86}Sr < 0.716$. The volcanic imprint is particularly evident in samples from McMurdo (Erebus volcano area) and Cape Crozier. These samples fall in the IInd Quadrant (Fig. 3b), which includes rocks derived from magma sources that are the residual solids after withdrawal of a partial melt from undifferentiated mantle (i.e., with higher Sm/Nd and lower Rb/Sr than the chondrite uniform reservoir).

Finally, South America has been detailed at high degree through 25 samples from the Pampas, Patagonia and Chilean Andes. Most of them present a signature restricted into the $0.7045 < {}^{87}Sr/{}^{86}Sr < 0.7130$ and $-5 < \varepsilon_{Nd}(0) < +3$ isotopic ranges (as can be observed in Fig. 4).

The comparison between the isotopic signature of the fine-grained South American samples (Chile and Argentina) and bibliographic data on *bulk* (all sizes) samples from Patagonian loesses (from Gallet et al., 1998; Grousset et al., 1992), Argentine continental shelf (from Basile et al., 1997), the Andean lavas and Andesites (from Hawkesworth et al., 1979; Francis et al., 1977; Futa and Stern, 1988) reported in Fig. 4 points out that the <5 μm fraction brings a Sr signature more radiogenic. This is confirmed also by the recent study of Smith et al. (2003).

When only the small-sized samples are taken into account, the whole ICD isotopic field is almost completely surrounded by the South American samples; this is not the case when the isotopic fields of the bulk PSA samples are considered (Basile et al., 1997).

3.3. The signature of the leached samples

The results of the leaching experiments are reported in Table 3. The ${}^{87}Sr/{}^{86}Sr$ ratios shift towards relatively higher values in the leached samples; the difference ($\Delta {}^{87}Sr/{}^{86}Sr$) between the leached and the unleached sample spans the interval $0.0002 < \Delta {}^{87}Sr/{}^{86}Sr < 0.0109$, and is on average 0.004. Neodymium shifts are higher than one epsilon unit only in four cases (A5, SA5, SA6, SA14), while for the rest of the samples, the difference between leached and unleached sample are negligible ($-0.6 < \Delta\varepsilon_{Nd}(0) < 0.9$).

4. Discussion

4.1. Dust flux to Dome C and Vostok in the last 220,000 years

The EPICA dust record for the late Pleistocene and Holocene periods evidences the atmospheric dust load was considerably higher in glacial cold periods than during interglacials. This evidence is widespread and unequivocally documented from many paleoclimate records of the Quaternary (see Kohfeld and Harrison, 2001 for a global overview). However, since the global increase in the atmospheric dust load was not globally uniform, it is important to validate the spatial significance of each record. Since major aerosol changes are governed by the same processes (e.g., sea level changes, extension of arid areas), the main glacial/interglacial changes in mineral aerosol can be confidently considered synchronous with respect to the Antarctic (Delmas and Petit, 1994) and can be adopted as stratigraphic markers; moreover, Jouzel et al. (1995) evidenced that the adjustment of Antarctic ice core chronologies through dust markers allows to refine synchronization of the glacial/interglacial isotopic (temperature) changes.

The comparison between the new EPICA dust record and that from the Vostok ice core (Petit et al., 1999) shows high coherency for the last 220,000 years, suggesting that each core is regionally significant with respect to the dust input to East Antarctica.

Assuming an average accumulation rate of 1.5 cm $year^{-1}$, the average dust fluxes are comparable between the two sites, and are ~975, ~750 and ~450 ng_{dust} cm^{-2} $year^{-1}$ in EPICA ice core and ~1000–1300, ~900–1000 and ~600–700 ng_{dust} cm^{-2} $year^{-1}$ in the Vostok ice core during stages 2, 4 and 6, respectively. The dust flux is ~40 ng_{dust} cm^{-2} $year^{-1}$ (~15 ppb in concentration) during both interglacials. Comparing the dust flux ratios for stages 2/4, we obtain 1.3 in EPICA and 1–1.4 in Vostok cores, and for stages 4/6, we obtain 1.6–1.7 in EPICA and 1.5 at Vostok. The slight differences could be justified by the different particle counter used for the analysis of the Vostok samples.

The high dust input of continental aerosol to the East Antarctic in glacial times reflects the enhanced

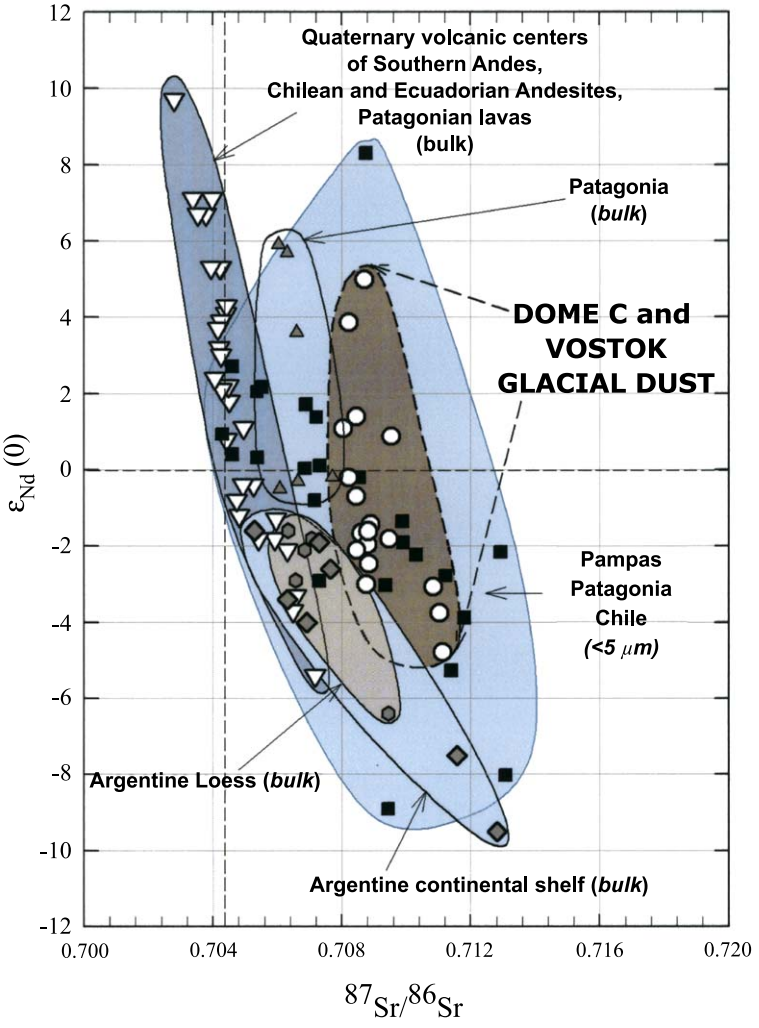

Fig. 4. Comparison between EPICA-Dome C and Vostok glacial dust field (dashed line) and the $^{87}Sr/^{86}Sr$ versus $\varepsilon_{Nd}(0)$ isotopic fields for South America samples from different bibliographic sources. Bulk (all size) samples from Andesites, Quaternary volcanic centers of the Southern Andes and Patagonian lavas have been taken from Hawkesworth et al. (1979) and Futa and Stern (1988), Argentine loess data (bulk) are from Gallett et al. (1998), Patagonian data (bulk) from Grousset et al. (1992) and the Argentine continental shelf data are from Basile et al. (1997). The isotopic field for the fine-grained (< 5 μm) south American samples (this work) is also reported. It can be observed that the latter encircles the whole IDC field and that the majority of the samples are concentrated in the $0.704 < {}^{87}Sr/^{86}Sr < 0.714$ and $+3 < \varepsilon_{Nd}(0) < -5$ interval.

dustiness of the atmosphere that was primarily linked to the enhanced aridity of continental areas and to the high wind speed, which favoured dust uplift (e.g., Petit et al., 1999). Moreover, the exposed lands were wider than today because of sea level lowering (e.g., Shackleton et al., 1983). These factors act in synergy since surface winds make soil surface drier, favouring dust mobilization, and ultimately mobilization by saltation and impaction (e.g., Smith et al., 2002). A crucial role in dust emission is played also by the typology and extent of vegetation cover, and by its seasonal and interannual variations, as evidenced by Tegen et al. (2002a,b). Finally, the hydrological cycle was reduced in cold periods, limiting washout processes en route (Yung et al., 1996).

A general overview of the environmental conditions in the Southern Hemisphere during the LGM and glacial periods suggests that all the continental areas are potential candidate sources for dust to East Antarctica. There are widespread paleoclimatic evi-

Table 3
Comparison between the leached and the unleached samples (<5 μm fraction) from New Zealand, Dry Valleys and South America

	$^{87}Sr/^{86}Sr$	$^{143}Nd/^{144}Nd$	$\varepsilon_{Nd}(0)$	$\Delta^{87}Sr/^{86}Sr$	$\delta\varepsilon_{Nd}(0)$	XRD <5 μm fraction calcite	Bulk sample, all sizes (reaction to HCl)
New Zealand							
NZ1	0.705183 (24)	0.512576 (11)	− 1.21				
NZ1—leached	0.705820 (29)	0.512580 (22)	− 1.13	0.0006	0.08	N	N
NZ2	0.709683 (19)	0.512442 (20)	− 3.82				
NZ2—leached	0.714248 (15)	0.512448 (17)	− 3.71	0.0046	0.12	N	N
NZ6	0.711190 (26)	0.512306 (17)	− 6.49				
NZ6—leached	0.722100 (18)	0.512305 (14)	6.50	0.0109	− 0.01	N	N
Dry Valleys							
A2	0.703194 (15)	0.512929 (07)	5.68				
A2—leached	0.703399 (17)	0.512928 (11)	5.66	0.0002	− 0.02	N	Y
A3	0.709797 (41)	0.512492 (08)	− 2.85				
A3—ached	0.713281 (16)	0.512521 (09)	− 2.28	0.0035	0.57	N	Y
A5	0.703357 (09)	0.512818 (08)	3.51				
A5—leached	0.708833 (14)	0.512678 (08)	0.78	0.0055	2.73	N	N
A9	0.715600 (14)	0.512129 (19)	− 9.93				
A9—leached	0.717688 (16)	0.512156 (18)	− 9.40	0.0021	0.53	N	Y
South America							
SA1	0.707320 (23)	0.512644 (09)	0.12				
SA1—leached	0.708600 (15)	0.512593 (26)	− 0.88	0.0013	− 0.99	Y	Y
SA2	0.708547 (19)	0.512628 (11)	− 0.20				
SA2—leached	0.710172 (12)	0.512598 (09)	− 0.78	0.0016	− 0.59	N	N
SA3	0.710311 (16)	0.512524 (15)	− 2.22				
SA3—leached	0.716666 (14)	0.512485 (11)	− 2.98	0.0064	− 0.76	Y	Y
SA4	0.709908 (21)	0.512541 (11)	− 1.89				
SA4—leached	0.715500 (10)	0.512528 (12)	− 2.15	0.0056	− 0.25	N	N
SA5	0.711218 (26)	0.512496 (14)	− 2.77				
SA5—leached	0.719937 (48)	0.512437 (11)	− 3.92	0.0087	− 1.15	N	N
SA6	0.709357 (22)	0.512483 (08)	− 3.02				
SA6—leached	0.714994 (12)	0.512422 (14)	− 4.21	0.0056	− 1.19	Y	Y
SA12	0.708620 (14)	0.512552 (14)	− 1.68				
SA12—leached	0.710109 (13)	0.512573 (09)	− 1.27	0.0015	0.41	N	N
SA14	0.711806 (21)	0.512439 (07)	− 3.88				
SA14—leached	0.716000 (18)	0.512353 (17)	− 5.56	0.0042	− 1.68	N	Y

Beside $^{87}Sr/^{86}Sr$, $^{143}Nd/^{144}Nd$ ($\pm 2\sigma \times 10^{-6}$ in brackets) and $\varepsilon_{Nd}(0)$, the leached–unleached difference (Δ) in $^{87}Sr/^{86}Sr$ and $\varepsilon_{Nd}(0)$ are reported. The last two columns indicate if calcite was detected through XRD analysis on the fine fraction (G. Roman-Ross, personal communication) and through test of effervescence with cold HCl on the bulk (all sizes) sample (N = no calcite; Y = yes).

dences of colder and drier conditions in glacial periods with respect to interglacials in the high latitudes of southern South America (e.g., Clapperton, 1993a,b), New Zealand (e.g., McGlone et al., 1993), as well as the whole Australian region (e.g., Bowler, 1978; Nanson et al., 1992). Sea level was ca. 120 m lower than the present (Shackleton et al., 1983), making much of the modern continental shelves exposed and Australia joined to Tasmania (e.g., Bowler, 1978). On the opposite, at the low latitudes of Chile (~ 27°S) and in southwestern southern Africa (20°S), glacials periods were wetter than interglacials (Stuut, 2001).

It is generally accepted that from glacial to interglacial stages the waxing and waning of the circum Antarctic sea ice may have forced the zone of moisture-bearing Westerlies to shift in latitude, thus influencing the regional climate of a large part of the Southern Hemisphere. While for South America, there is general agreement about the equatorward displacement of the Westerlies during the LGM (e.g., Wright et al., 1993), for the Australian region, the situation is more controversial. Earlier reconstructions (e.g., Harrison et al., 1984) suggested an equatorial displacement of the subtropical high pressure belt and the Westerlies. This scenario, however, did not account for the aridity in Tasmania and in southern Australia at 18 kyears BP; Harrison and Dodson (1993) proposed a different interpretation of the paleovegetation and paleohydrological data hypothesizing a poleward rather than equatorward displacement of the Westerlies and a southward expansion of the subtropical high pressure belt. Their scenario, which justifies the exclusion of Tasmania from the year-round Westerlies, is supported also by the dynamics of the transition to the Holocene climate, that occurred at ca. 12 kyears BP: Wetter conditions were registered first in Tasmania and subsequently in Southeast Australia, indicating a progressive equatorward advance of the Westerlies belt during the LGM/Holocene transition.

An aeolian dust record from the Tasman Sea (Hesse and McTainsh, 1999) evidences a decrease in the terrigenous flux from the LGM to the Holocene, but surprisingly without significant change in particle size. The higher dustiness of the last glacial period was therefore attributed to enhanced continental aridity and to the expansion of the exposed land (i.e., higher dust availability) rather than increased wind strength.

The climatic and environmental conditions during the LGM in every continental domain of the Southern Hemisphere were very different to those of the Holocene and present day.

The expansion of the polar front played a key role, but the geometry of its displacement is not well known, and it was not necessarily symmetrical in the circum Antarctic. In this context, the determination of the geographical provenance of dust to the East Antarctic can help to better assess the atmospheric dynamics at that time.

4.2. Deciphering the information of dust tracers: the $^{87}Sr/^{86}Sr$ versus $^{143}Nd/^{144}Nd$ method

The use of geochemical *tracers* for the identification of the dust origin is a powerful tool, provided that some conditions are satisfied. In the following paragraphs we will discuss in detail these points, but, first, a general definition of the concept of dust tracer and its significance must be done.

A tracer for dust (isotopic, mineralogical or other else) should be (1) representative for a geographical region, (2) distinctive for that region with respect to other areas and (3) conservative from the source to the sink. Moreover, as previously underlined (Section 2.2.1), the PSA samples must be adequately collected in order to be representative for a geographical region. The changes in the mineralogical and isotopic composition occurring in function of the particle size as well as an eventual contribution from carbonates are also factors that have to be taken in consideration.

4.2.1. The use of $^{87}Sr/^{86}Sr$ versus $^{143}Nd/^{144}Nd$ isotopic ratios

The use of naturally occurring stable and radiogenic isotopes as dust tracers had first applications in oceanography (e.g., Grousset et al., 1988), and was subsequently used to investigate the origin of aeolian dust in Antarctica (Grousset et al., 1992). Biscaye et al. (1997) associated Sr and Nd tracers to the $^{206,207,208}Pb/^{204}Pb$ ratios and a mineralogical indicator based on the relative abundance of kaolinite and chlorite clays. On the other hand, the REE profile seems to be an unsuitable tracer for mixed materials like loesses and sediments, since the profile resembles that of the upper

continental crust (Gallet et al., 1998). Grousset et al. (1992) and Basile et al. (1997) evidenced the same flat pattern is typical in ice core dust. There is no ideal tracer, and each approach has its limits.

In this work, we use $^{87}Sr/^{86}Sr$ versus $^{143}Nd/^{144}Nd$ isotopic ratios as tracers and compare the signature at the source with the signature at the sink. The basic principle is that soils and sediments keep the Sr–Nd isotopic imprint of rock(s) from which they derive, which, in turn, depends on lithology and geologic age (Basile, 1997). The significance of the isotopic signature of mixed sediments is primarily *geographical* and not necessarily *geological*, since different types of rocks can have contributed to the formation of the detrital sediments in the PSA.

This approach, however, presents some limits: The PSA samples collected do not pretend to be exhaustive of all potential source regions, and, moreover, we did not sample in this study the areas forming continental shelves at present day, which were partially exposed during glacial periods.

4.2.2. Particle size and isotopic signature

To use the Sr–Nd tracer for the identification of dust transported long range, it has to be taken into consideration that the atmospheric transport leads to particle size selections. Therefore, a basic question arises: Is there necessity to take this effect into account in defining the isotopic signature of the PSA samples? In other terms, has the fine fraction of PSA samples the equivalent isotopic signature that the total fraction (bulk) of PSA samples?

Three main processes can be reviewed in theory to answer that problem:

(1) In a given rock, all the minerals have their own Rb and Sm initial concentration. Over geological time, radioactive decay leads to specific isotopic $^{87}Sr/^{86}Sr$ and $^{143}Nd/^{144}Nd$ signatures for each mineral. This property is at the base of Sm–Nd and Rb–Sr geochronology. Thus, any process which is susceptible of sorting minerals after any desegregation of the rock will lead to an isotopic fractionation regarding to the initial whole rock.

(2) The rock also can be subjected to two types of alteration processes. The physical weathering (like grinding in glacial environments) affects minerals in a different way according to their hardness: For example, biotite can be more easily grounded in fine fraction than quartz. On the other hand, the chemical alteration (weathering by running water) will also affect the minerals differentially: For example, Ca-feldspars can be completely dissolved by weathering while neighbored quartz is not affected. These two types of alteration processes can thus lead to granulometric and mineralogic transformations of the initial rock and can induce, in case of size selection, isotopic fractionation.

(3) During weathering, the less soluble elements can precipitate in situ and form ‘‘neoformed phases’’, which are in general clay-sized minerals. As Sr is highly soluble compared to Rb, neoformed phases will be enriched in Rb and will acquire a high $^{87}Sr/^{86}Sr$ over geological times. Therefore, the clay-sized fraction containing neoformed phases will have a more radiogenic Sr signature than the clay-sized fraction of the unweathered rock.

In conclusion, each of the above-mentioned processes and their combination leads to a different isotopic signature between the clay-sized fraction and the bulk fraction of a PSA sample. Besides these theoretical processes, some authors have, moreover, measured isotopic differences between size fractions (e.g., Derry and France-Lanord, 1996, see Basile, 1997; Smith et al., 2003 and references therein). For example, isotopic fractionation between different size fractions can range from 0.720 to 0.752 in $^{87}Sr/^{86}Sr$ (Derry and France-Lanord, 1996) and from -18 to -5 in $\varepsilon_{Nd}(0)$ (Goldstein et al., 1984). Thus, to use isotopic ratios signatures as tracers, one has to compare dust of equivalent size at the source and at the end of the transport. As mineral particles in Antarctic ice are smaller than 5 μm (Delmonte et al., 2002), the signature of PSA has to be measured in the same size range.

4.2.3. The Sr contribution from carbonates

The mineral particles and amorphous materials that constitute a PSA sample can be mixed with authigenic compounds as carbonates and sulfates that are typical in soils or sedimentary deposits. The $^{87}Sr/^{86}Sr$ ratio of these formations, which are extremely widespread in arid and semiarid climates, depends on the source of calcium carbonate in the host material.

Various studies (e.g., Chiquet et al., 1999) have shown that calcium can derive either from in situ weathering of the parent rocks or from an allochtonous source, which can be continental calcareous

aerosol transported by wind or seawater. In the latter case, the Sr isotopes keep the seawater signature, and for this reason, they are commonly used as tool for investigation of Ca origin in carbonate accumulations (Hamidi et al., 1999).

The Sr concentration in carbonates is very high (>600 ppm), and even a small percentage of $CaCO_3$ in a PSA sample will influence the signature of the remaining (aluminosilicate) fraction. With respect to this problem, previous studies followed two different approaches for ICD–PSA comparison.

In Greenland, the dust fluxes are higher than in Antarctica of a factor of 10, and the carbonate contribution is important, making the ice pH slightly alkaline (Steffensen, 1997). Therefore, a "leached–leached" strategy of comparison has been adopted (Biscaye et al., 1997): Both ice and source samples have been decarbonated and the residual aluminosilicate fractions compared.

For Antarctica, the situation is different; there is evidence that dust reaching East Antarctica has no carbonates (DeAngelis et al., 1992). The pH of ice is slightly acid (~ 5.5) both for glacial and interglacial periods, and the absence of carbonates in particles extracted from the ice is confirmed also by some analysis made on some filtered dust (>0.4 μm) from the Old Dome C core, evidencing a Ca/Al ratio impoverished with respect to the upper continental crust (De Angelis, personal communication). Moreover, a leaching test performed on a glacial dust sample from Antarctic ice (Delmonte, in preparation) has shown no differences in Sr between the leached and the unleached fractions.

Calcite, however, could have been present to a certain extent at the source and during the first stages of the aeolian phase, and totally lost en route.

These considerations lead previous authors (Basile et al., 1997) to adopt an unleached–unleached strategy for Antarctic ice. In the present study, we basically follow this latter approach, but performed also leaching tests on some PSA samples. The results show that the leaching procedure induced shifts in the isotopic composition of Sr isotopes systematically towards more radiogenic values.

In order to check if the differences between leached and unleached sample were due to the presence of carbonates, we used X-ray diffraction analysis (detection limit 5%) and effervescence to cold HCl. Qualitative results are reported in Table 3. X-ray diffraction measurements were performed on the fine fraction of PSA samples. They showed calcite only in three samples (SA1, SA3, SA6, G. Roman-Ross, personal communication). A slightly larger group of samples (mainly the South Africa and the Dry Valleys groups) evidenced effervescence to cold HCl on the bulk sample before size separation. This difference between bulk and fine fractions could be due to the presence of calcite only in the >5 μm fraction or to the dissolution of $CaCO_3$ during sample suspension in MilliQ water for size selection. Another possibility is that the carbonates could be present indeed, but in a quantity below the detection limit of XRD.

However, whether the sample contains calcite or not, a shift in the isotopic composition of the samples has been observed on all kinds of samples. The leaching procedure is supposed to remove carbonates from samples, but it cannot be excluded a possible bias effect on Sr (and possibly Nd) kept by other phases like the labile volcanic glasses for instance, or the clay minerals where strontium resides adsorbed on mineral surfaces and in interlayer sites.

Actually, clays are the dominant mineral phase in East Antarctic ice (Gaudichet et al., 1986, 1988) and represent about 40% of the total number of particles. Crystalline silica and feldspars, on the opposite, are present in lower amounts (about 15% for each group). Among clays, illite is the most abundant (>60%) in Vostok ice (Gaudichet et al., 1992), while smectite, chlorite and kaolinite were present in minor proportions. If present, the possible isotopic bias introduced by the leaching procedure on clay minerals is difficult to quantify, and the measure of both leached and unleached fine-grained samples would be recommended therefore for the estimation of the maximum $\Delta^{87}Sr/^{86}Sr$ for carbonate contribution. In this study, we adopted the unleached–unleached strategy of comparison, but the Sr shift for carbonate contribution has been considered.

In conclusion, the isotopic $^{87}Sr/^{86}Sr$ versus $^{143}Nd/^{144}Nd$ fingerprint can be used as tracer for dust if the sample can be considered representative for a geographical region, if it is analyzed in the equivalent size range of the dust at the sink, and if the $\Delta^{87}Sr/^{86}Sr$ for carbonate contribution is taken into account. Despite all the limits cited above, however, the recognition of the geographical provenance of dust

through its isotopic fingerprint can be considered a robust method (Basile, 1997; Biscaye et al., 1997).

4.3. The identification of the geographical source for Antarctic dust in glacial periods

The isotopic fields defined by the EPICA-Dome C and Vostok dust (Fig. 3a) are almost the same between the two sites and for all glacial periods investigated in this work (stage 6 for Vostok and stages 2, 4, 6 for Dome C), and in previous ones (stages 4, 6, 8, 10, 12 for Vostok, from Basile, 1997; stage 2 for Dome C, from Grousset et al., 1992; Basile et al., 1997).

This suggests common dominant source region(s) for East Antarctic dust during the cold periods of the late Pleistocene.

The Antarctic ICD signature appears very different from South Africa and Australia, and these two regions—even if poorly documented in this study—can be excluded as dominant sources in glacial periods. Their isotopic signature (Fig. 3b) reflects their (first-order) geological nature, since they are a portion of a large Precambrian shield. The isotopic fields that we traced are based on a very limited number of samples, nevertheless, they are globally similar to the fields previously traced by Basile (1997) and Grousset et al. (1992) on the basis of bulk (all sizes) samples, and that allowed the authors to exclude them as principal sources for aeolian dust reaching Antarctica in glacial periods.

Antarctic ice dust signature is situated in the overlap region between New Zealand, the Dry Valleys and southern South America; if a possible contribution from all these three sources cannot be excluded from isotopic measurements only, many complementary arguments help in the interpretation.

The final conclusions drawn from the data do not change when the $^{87}Sr/^{86}Sr$ shift for leaching is considered, but the isotopic fields for the sources result slightly enlarged (see figure in Delmonte et al., 2003).

New Zealand is a long and narrow twin island lying south of 35°S (Fig. 1), characterised by latitudinal and longitudinal climatic and environmental differences. Southern regions are primarily under the influence of the westerly winds, while the northern regions extend into the subtropical ridge of high pressures (e.g., McGlone et al., 1993). Moreover, the South Island is traversed southwest–northeast by the southern Alps and contrasting temperature and precipitation regimes exist in function of longitude. During LGM windiness increased in the South Island, ice cover was extended to the coastal lowlands of the central west coast and some loess deposits were formed (McGlone et al., 1993).

New Zealand is a potential source for dust in Antarctica, but its surface extent is very limited, therefore, it is unlikely the main factor responsible for the high dust flux in glacial periods. If it was the case, moreover, it would be surprising that any contribution from the nearby large deserts of Australia is detected. Finally, the absence of tephra layers from the Taupo Volcanic Zone in the Vostok ice core for the last 420,000 years (Basile et al., 2001) also suggests that this atmospheric path is quite unfavourable.

The non-glaciated area of the Dry Valleys of coastal Antarctica is also unlikely the principal dust source in glacial times. First, ice-free areas were less extended than today, and the glacier's fronts were closer to the coast (Denton and Hughes, 2002). In an environment of this kind, with limited seasonal variations and hydrological cycle, the primary production of fine-grained dust occurs quasi exclusively through mechanical alteration of primary rocks, and it is very limited. Second, the strong catabatic winds blowing off the East Antarctic Plateau carry the mineral aerosol towards the ocean (Schwerdtfeger, 1970). In order to be transported back to the high plateau, the particles must be uplifted into the middle–high troposphere and finally brought back into the continent; this kind of transport is very unlikely.

A further argument suggesting the atmospheric transport from West to East Antarctica is not usual is the presence of only one volcanic tephra layer from Marie Byrd Land volcanoes in the Vostok ice core (Basile et al., 2001) and one in the Dome C core (Kyle et al., 1981). This volcanic province of West Antarctica has been very active in the late Pleistocene, as evidenced by the ~2000 visible ash layers of the Byrd ice core (Gow and Williamson, 1971).

Finally, the Dry Valleys region is typically characterized by the presence of considerable quantities of salts deriving from the first stages of chemical weathering of rocks, like gypsum and carbonates. The latter are very common (Campbell and Claridge, 1987), but

they are not found in Antarctic ice (DeAngelis et al., 1992). If weathering during transport through reactions with acid aerosol are likely, it is hard to believe that these should be capable to remove the totality of these components during the short path described above.

Southern South America was likely the dominant source for East Antarctic dust in glacial times, as already evidenced by Basile (1997) and Grousset et al. (1992). This region extends south of 40°S, and is under the continuous flux of the Westerlies. Moisture is largely removed from the air masses as they pass over the Andes, and the eastern side of the mountain chain in an extensive rain-shadow zone with very low annual rainfall (Clapperton, 1993a,b).

South America has geomorphologic and environmental conditions favourable for primary production, mobilization and transport of fine-grained dust. During cold periods, the continental glaciers enhanced rock alteration, providing sandy and silty particles. These can be either a primary source for long-range dust or can be available for mobilization and fluvial or aeolian transport to another site topographically suitable for concentration of sediments. It is the case for example of the plains east of the cordillera, where fluvioglacial deposits, alluvial fans and widespread loess and loess-like deposits have been generated.

These sediments derive from the andesites and the volcanic rocks of the cordillera and keep the typical signature of their parent rock, which distinguish Patagonian loess from all other loess deposits around the world (Gallet et al., 1998).

In Fig. 4, all the available Sr–Nd bibliographic data from southern South America are reported. Andesites and lavas are very low radiogenic in Sr and span a wide range of $\varepsilon_{Nd}(0)$. The argentine continental shelf keeps almost the same signature of the loess (Gallet et al., 1998, Fig. 4) since the primary material is the same. In glacial periods, when the sea level was lower, the shelf was exposed and therefore it must be considered also as potential source for dust.

The slight offset towards more radiogenic Sr of the Antarctic ICD samples with respect to bulk (all sizes) Argentine loess was attributed by Basile et al. (1997) either to a possible contribution of another source, like Australia or South Africa (estimated 10–15% maximum) or to a grain-size effect (see Section 4.2.2). The new isotopic field defined in this work on the basis of the signature of the fine fraction of South American samples, encompasses the Antarctic dust's one (Fig. 4), and favors the latter hypothesis.

A southern South American origin for glacial dust was first suggested by Gaudichet et al. (1986) on the basis of mineralogical data, and confirmed by Grousset et al. (1992) on the basis of geochemical analysis, subsequently developed by Basile et al. (1997) and Basile (1997). This study confirms that dust on the East Antarctic plateau (Dome C and Vostok) has the same atmospheric trajectory during all the studied glacial periods. The favourable atmospheric pathway from that region arises also from the evidence that all volcanic tephra layers in the Vostok ice core originate from South Atlantic volcanoes of the South Sandwich Island and the Antarctic Peninsula (Basile et al., 2001).

Recent atmospheric circulation models for LGM (Lunt and Valdes, 2002) support this hypothesis and estimate the Patagonian source (31–50°S) as about 620% stronger than today, when the decreased soil moisture and vegetation and the increase in land area due to sea level fall are considered. Moreover, dust transport simulation for the LGM (Andersen, 1998) evidenced from spring to fall a preferential advection from South America.

The climatic and environmental changes occurred in the Quaternary between cold and warm stages modified sensibly the conditions in continental areas: vegetation development and pedogenesis, sea level rise, change in hydrological conditions and wind strength are examples. All these factors can affect sensibly the strength of the source regions, as the huge decrease in dust concentration in the Holocene and in stage 5.5 evidenced. Moreover, significant changes in atmospheric dust transport between the Last glacial period and the Holocene have been observed in the EPICA-Dome C ice core (Delmonte et al., 2002). These observations let an open question about the dust provenance in interglacial epochs.

5. Conclusion

The comparison of two dust profiles from the deep East Antarctic ice cores of EPICA-Dome C and Vostok

shows a strict similarity for the last 220,000 years, suggesting the dust input has been rather uniform into the Eastern Plateau in the late Quaternary.

The Sr–Nd signature of glacial ice core dust evidences a dominant source that is common at both sites and throughout all cold periods.

The isotopic signature of the PSA of the Southern Hemisphere has been refined in the <5 μm fraction and a new database suitable for comparison with the ice core dust has been obtained. The signature New Zealand and the Antarctic Dry Valleys, documented for the first time, overlaps the South American one, but many complementary arguments allow to estimate their possible contribution negligible.

The carbonate contribution to the Sr signature of the sources is taken also into consideration, and leaching tests have been performed on some samples. Assuming the leaching method suitable for removing only the carbonate contribution, the Sr shifts observed make the PSA isotopic fields larger but do not change the final interpretation of the data.

The southern South American regions of the Pampas and Patagonia and possibly also the Argentine exposed continental shelf appear the dominant sources for dust in cold periods.

These results show a remarkable uniformity in the first-order dynamics of dust reaching the East Antarctica plateau, in terms of dust flux and geographical provenance.

Acknowledgements

The authors wish to thank Prof. F.Previtali, Dr. R.Comolli, Dr. M.Zaraté, Dr. A. Aristarain, Dr. A. Whintle, P.Hesse and many other anonymous providers of PSA samples.

The authors wish to thank both the Max Plank Institute of Mainz, Germany, and the CEREGE laboratory in Aix en Provence, France, for permitting access to laboratory facilities, and in particular Mr. R. Jotter in Mainz, Mr. W.Barthelemy and Dr. K.Tachikawa (CEREGE) for their help and useful suggestions. Thanks are also addressed to P.Biscaye and M. De Angelis for useful discussions, to Dr. Gabriela Roman-Ross for performing XRD analysis on PSA samples and to O.Leroux for helping in Coulter Counter measurements. Special thanks to K. Kohfeld and A. Bory, who reviewed the manuscript, for their useful suggestions and comments.

This work was carried out within the framework of a Project on Glaciology and Paleoclimate of the Programma Nazionale di Ricerche in Antartide (PNRA) and was supported by ENEA in Italy and in France by CNRS Project VAGALAM from PNEDC.

This work is a contribution to the "European Project for Ice Coring in Antarctica" (EPICA), a joint ESF (European Science Foundation)/EC scientific programme, funded by the European Commission under the Environmental and Climate Programme (1994–1998) contract ENV4-CT95-0074 and by national contributions from Belgium, Denmark, France, Germany, Italy, the Netherlands, Norway, Sweden, Switzerland and the United Kingdom. This is EPICA publication no. 73.

B. Delmonte thanks the Scientific Committee for Antarctic Research (SCAR) for awarding the Prince of Asturias fellowship 2003.

References

Andersen, K.K., 1998. Simulations of atmospheric dust in the glacial and interglacial climate. PhD thesis, University of Copenhagen, Denmark.

Basile, I., 1997. Origine des aérosols volcaniques et continentaux de la carotte de glace de Vostok (Antarctique). PhD thesis Université Joseph Fourier—Grenoble I, France.

Basile, I., Grousset, F.E., Revel, M., Petit, J.R., Biscaye, P.E., Barkov, N.I., 1997. Patagonian origin of glacial dust deposited in East Antarctica (Vostok and Dome C) during glacial stages 2, 4 and 6. Earth Planet. Sci. Lett. 146, 573–589.

Basile, I., Petit, J.R., Touron, S., Grousset, F.E., Barkov, N.I., 2001. Volcanic tephra in Antarctic (Vostok) ice-cores: source identification and atmospheric implications. J. Geophys. Res. 106 (D23), 31915–31931.

Biscaye, P.E., Dasch, E.J., 1971. The rubidium–strontium isotope system in deep sea sediments: Argentine basin. J. Geophys. Res. 76, 5087–5096.

Biscaye, P.E., Grousset, F.E., Revel, M., Gaast, S.V., Zielinski, G.A., Vaars, A., Kukla, G., 1997. Asian provenance of glacial dust (stage 2) in the Greenland Ice Sheet Project 2 ice core, summit, Greenland. J. Geophys. Res. 102 (C12), 26765–26781.

Bogdanovski, O., 1997. Development of highly-sensitive techniques for Sm–Nd isotopic analysis and their application to the study of terrestrial and extraterrestrial objects. PhD thesis, Johannes Gutenberg Universitat, Mainz, Germany.

Bowler, J.M., 1978. Glacial age aeolian events at high and low latitudes: a Southern Hemisphere perspective. In: Van Zinderen Bakker, E.M. (Ed.), Antarctic Glacial History and World Palaeoenvironments. Balkema, Rotterdam, pp. 149–172.

Campbell, I.B., Claridge, G.G.C., 1987. Antarctica: Soils, Weathering Processes and Environment Elsevier, Amsterdam.

Chiquet, A., Michard, A., Nahon, D., Hamelin, B., 1999. Atmospheric input vs in situ weathering in the genesis of calcretes: an Sr isotope study at Gàlvez (Central Spain). Geochim. Cosmochim. Acta 63 (3–4), 311–323.

Clapperton, C.M., 1993a. Nature of environmental changes in South America at the Last Glacial Maximum. Palaeogeogr. Palaeoclimatol. Palaeoecol. 101, 189–208.

Clapperton, C.M., 1993b. Quaternary Geology and Geomorphology of South America. Elsevier, Amsterdam.

DeAngelis, M., Barkov, N.I., Petrov, V.N., 1992. Sources of continental dust over Antarctica during the last glacial cycle. J. Atmos. Chem. 14, 233–244.

Delmas, R., Petit, J.R., 1994. Present Antarctic aerosol composition: a memory of ice age atmospheric dust? Geophys. Res. Lett. 21, 879–882.

Delmonte, B., Petit, J.R., Maggi, V., 2002. Glacial to Holocene implications of the new 27,000-year dust record from the EPICA Dome C (East Antarctica) ice core. Clim. Dyn. 18 (8), 647–660.

Delmonte, B., Petit, J.R., Basile-Doelsch, I., Michard, A., Gemmiti, B., Maggi, V., Revel-Rolland, M., 2003. Refining the isotopic (Sr–Nd) signature of potential source areas for glacial dust in East Antarctica. J. Physique IV (107), 365–368.

Denton, G.H., Hughes, T.J., 2002. Reconstructing the Antarctic ice sheet at the last glacial maximum. Quat. Sci. Rev. 21, 365–433.

DePaolo, D.J., Wasserburg, G.J., 1976. Nd isotopic variations and petrogenetic models. Geophys. Res. Lett. 3, 249–252.

Derry, L.A., France-Lanord, C., 1996. Neogene Hymalayan weathering history and river $^{87}Sr/^{86}Sr$: impact on the marine Sr record. Earth Planet. Sci. Lett. 142, 59–74.

Francis, P.W., Moorbath, S., Thorpe, R.S., 1977. Strontium isotope data for recent andesites in Ecuador and North Chile. Earth Planet. Sci. Lett. 37, 197–202.

Fung, I., Meyn, S., Tegen, I., Doney, S.C., John, J., Bishop, J.K.B., 2000. Iron supply and demand in the upper ocean. Glob. Biogeochem. Cycles 14, 281–296.

Futa, K., Stern, C.R., 1988. Sr and Nd isotopic and trace element composition of Quaternary volcanic centers of the southern Andes. Earth Planet. Sci. Lett. 88, 253–262.

Gallet, S., Jahn, B., Lanoe, B.V.V., Dia, A., Rossello, E., 1998. Loess geochemistry and its implications for particle origin and composition of the upper continental crust. Earth Planet. Sci. Lett. 156, 157–172.

Gaudichet, A., Petit, J.R., Lefevre, R., Lorius, C., 1986. An investigation by analytical transmission electron microscopy of individual insoluble microparticles from Antarctic (Dome C) ice core samples. Tellus (38B), 250–261.

Gaudichet, A., Angelis, M.D., Lefevre, R., Petit, J.R., Korotkevitch, Y.S., Petrov, V.N., 1988. Mineralogy of insoluble particles in the Vostok Antarctic ice core over the last climatic cycle (150 Kyr). Geophys. Res. Lett. 15 (13), 1471–1474.

Gaudichet, A., De Angelis, M., Jossasume, S., Petit, J.R., Korotkevitch, Y.S., Petrov, V.N., 1992. Comments on the origin of dust in East Antarctica for present and ice age conditions. J. Atmos. Chem. 14, 129–142.

Goldstein, S.L., O'Nions, R.K., Hamilton, P.J., 1984. A Sm–Nd isotopic study of atmospheric dusts and particulates from major river systems. Earth Planet. Sci. Lett. 70, 221–236.

Gow, A.J., Williamson, T., 1971. Volcanic ash in the Antarctic ice sheet and its possible climatic implications. Earth Planet. Sci. Lett. 13, 210–218.

Grousset, F.E., Biscaye, P.E., Zindler, A., Prospero, J.M., Chester, R., 1988. Neodymium isotopes as tracers in marine sediments and aerosols: North Atlantic. Earth Planet. Sci. Lett. 87, 367–378.

Grousset, F.E., Biscaye, P.E., Revel, M., Petit, J.R., Pye, K., Jossaume, S., Jouzel, J., 1992. Antarctic (Dome C) ice-core dust at 18 k.y. B.P.: isotopic constraints and origins. Earth Planet. Sci. Lett. 111, 175–182.

Hamidi, E.M., Nahon, D., McKenzie, J.A., Michard, A., Colin, F., Kamel, S., 1999. Marine Sr (Ca) input in Quaternary volcanic rocks weathering profiles from the Mediterranean coast of Morocco: Sr isotopic approach. Terra Nova 11, 157–161.

Harrison, S.P., Dodson, J., 1993. Climates of Australia and New Guinea since 18,000 yr B.P. In: Wright, H.E., Kutzbach, J.E., Webb III, T., Ruddiman, W.F., Street-Perrott, F.A., Bartlein, P.J. (Eds.), Global Climates Since the Last Glacial Maximum. Minnesota press, Minneapolis, pp. 265–293.

Harrison, S.P., Metcalfe, S.E., Pittock, A.B., Roberts, C.N., Salinger, N.J., Street-Perrott, F.A., 1984. A climatic model of the last glacial/interglacial transition based on palaeotemperature and palaeohydrological evidence. In: Vogel, J.C. (Ed.), Late Cainozoic Palaeoclimates of the Southern Hemisphere. Balkema, Rotterdam, pp. 21–34.

Hawkesworth, C.J., Norry, M.J., Roddick, J.C., Baker, P.E., 1979. $^{143}Nd/^{144}Nd$, $^{87}Sr/^{86}Sr$, and incompatible element variations in calc-alkaline andesites and plateau lavas from South America. Earth Planet. Sci. Lett. 42, 45–57.

Hesse, P., McTainsh, G.H., 1999. Last glacial maximum to early holocene wind strength in the mid-latitudes of the southern hemisphere from aeolian dust in the Tasman sea. Quat. Res. 52, 343–349.

Hutchins, D.A., Brunland, K.W., 1998. Iron-limited diatom growth and Si:N uptake ratios in a coastal upwelling regime. Nature 393, 561–564.

Intergovernmental Panel on Climate Change (IPCC), 2001. Climate Change 2001. Cambridge Univ. Press, New York.

Jacobsen, S.B., Wasserburg, G.J., 1980. Sm–Nd isotopic evolution of chondrites. Earth Planet. Sci. Lett. 50, 139–155.

Jouzel, J., Vaikmae, R., Petit, J.R., Martin, M., Duclos, Y., Stievenard, M., Lorius, C., Toots, M., Melières, M.A., Burckle, L.H., Barkov, N.I., Kotlyakov, V.M., 1995. The two-step shape and timing of the last deglaciation in Antarctica. Clim. Dyn. 11, 151–161.

Jouzel, J., Masson, V., Cattani, O., Falourd, S., Stievenard, M., Stenni, B., Longinelli, A., Johnsen, S.J., Steffensen, J.P., Petit, J.R., Schwander, J., Souchez, R., 2001. A new 27 kyr high resolution East Antarctic climate record. J. Geophys. Res. 28, 3199–3202.

Kohfeld, K., Harrison, S.P., 2001. DIRTMAP: the geological record of dust. Earth-Sci. Rev. 54, 81–114.

Kyle, P.R., Jezek, P.A., Thompson, E.M., Thompson, L., 1981. Tephra layers in the Byrd Station ice core and the Dome C

ice core, Antarctica and their climatic importance. J. Volcanol. Geotherm. Res. 11, 29–39.
Lorius, C., Merlivat, L., Jouzel, J., Pourchet, M., 1979. A 30000 years isotope climatic record from Antarctic ice. Nature 280, 644–648.
Lunt, D.J., Valdes, P.J., 2002. Dust deposition and provenance at the Last Glacial Maximum and present day. Geophys. Res. Lett. 29 (22), 2085–2089.
Mahowald, N., Kohfeld, K., Hansson, M., Balkanski, Y., Harrison, S.P., Prentice, I.C., Schulz, M., Rodhe, H., 1999. Dust sources and deposition during the Last Glacial Maximum and current climate: a comparison of model results with paleodata from ice cores and marine sediments. J. Geophys. Res. 104 (D13), 15895–15916.
McGlone, M.S., Salinger, M.J., Moar, N.T., 1993. Paleovegetation studies of New Zealand's climate since the Last Glacial Maximum. In: Wright, H.E., Kutzbach, J.E., Webb III, T., Ruddiman, W.F., Street-Perrott, F.A., Bartlein, P.J. (Eds.), Global Climates Since The Last Glacial Maximum. Minnesota Press, Minneapolis, pp. 294–317.
Nanson, G.C., Chen, X.Y., Price, D.M., 1992. Lateral migration, thermoluminescence chronology and colour variation of longitudinal dunes near Birdsville in the Simpson Desert, central Australia. Earth Surf. Processes Landf. 17, 807–819.
Petit, J.R., Jouzel, J., Raynaud, D., Barkov, N.I., Barnola, J.M., Basile, I., Bender, M., Chappellaz, J., Davis, M., Delaygue, G., Delmotte, M., Kotlyakov, V.M., Legrand, M., Lipenkov, V.Y., Lorius, C., Pépin, L., Ritz, C., Saltzman, E., Stievenard, M., 1999. Climate and atmospheric history of the past 420,000 years from the Vostok ice core, Antarctica. Nature 399, 429–436.
Prospero, J.M., Ginoux, P., Torres, O., Nicholson, S.E., 2002. Environmental characteristics of global sources of atmospheric soil dust derived from the NIMBUS-7 TOMS absorbing aerosol product. Rev. Geophys. 40 (2). doi:10.1029/2000RG000092
Schwander, J., Jouzel, J., Hammer, C.U., Petit, J.R., Udisti, R., Wolff, E., 2001. A tentative chronology for the EPICA Dome Concordia ice core. Geophys. Res. Lett. 28, 4243–4246.
Schwerdtfeger, W., 1970. The Climate of the Antarctic. Elsevier, Amsterdam.
Shackleton, N.J., Imbrie, J., Hall, M.A., 1983. Oxygen and carbon isotope record of East Pacific core V19-30: implications for the formation of deep water in the late Pleistocene North Atlantic. Earth Planet. Sci. Lett. 65, 233–244.
Smith, B.J., Wright, J.S., Whalley, W.B., 2002. Sources of non-glacial, loess-size quartz silt and the origins of "desert loess". Earth-Sci. Rev. 59, 1–26.
Smith, J., Vance, D., Kemp, R.A., Archer, C., Toms, P., King, M., Zarate, M., 2003. Isotopic constraints on the source of Argentinian loess—with implications for atmospheric circulation and the provenance of Antarctic dust during recent glacial maxima. Earth Planet. Sci. Lett. 212, 181–196.
Steffensen, J.P., 1997. The size distribution of microparticles from selected segments of the GRIP ice core representing different climatic periods. J. Geophys. Res. 102 (C12), 26755–26763.
Stuut, J.B.W., 2001. Late Quaternary southwestern African terrestrial-climate signals in the marine record of Walvis Ridge, SE Atlantic Ocean. PhD Utrecht University, The Netherlands.
Swap, R.M., Garstang, M., Greco, S., Talbot, R., Kallberg, P., 1992. Saharan dust in the Amazon basin. Tellus, Ser. B Chem. Phys. Meteorol. 44, 133–149.
Taylor, S.R., McLennan, S.M., 1985. The Continental Crust: Its Composition and Evolution Blackwell, London.
Tegen, I., Harrison, S.P., Kohfeld, K., Prentice, I.C., 2002a. Impact of vegetation and preferential source areas on global dust aerosol: results from a model study. J. Geophys. Res. 107 (D21), 4576–4603.
Tegen, I., Harrison, S.P., Kohfeld, K.E., 2002. Modeling the role of mineral aerosols in global climate cycles. EOS 36 (395, 400).
Wright, H.E., Kutzbach, J.E., Webb III, T.W., Ruddiman, W.F., Street-Perrott, F.A., Bartlein, P.J., 1993. Global Climates Since The Last Glacial Maximum. University of Minnesota Press, Minneapolis. 550 pp.
Yung, Y.L., Lee, T., Wang, C.H., Shieh, Y.T., 1996. Dust: a diagnostic of the hydrologic cycle during the Last Glacial Maximum. Science 271, 962–963.

Barbara Delmonte obtained her University Degree in Environmental Sciences at the University of Milano (Italy) in November 1998, with a master's degree in Glaciology and Meteorology. She devoted afterwards her research interests to paleoclimate reconstructions from Antarctic ice cores working in the framework of the European Project for Ice Coring in Antarctica (EPICA) and participating to the XVII Italian Antarctic Expedition in Dome Concordia. B. Delmonte is now ending her PhD in Polar Sciences in co-agreement between Italy (University of Siena) and France (University Joseph Fourier, Grenoble). She obtained the Prince of Asturias 2003 Prize from the Scientific Committee for Antarctic Research (SCAR).